PENSOFT

SENCKENBERG
NATURE RESEARCH

Leibniz
Association

Secondary sexual traits and lineage diversification in the giant blister beetle *Berberomeloe insignis* (Coleoptera: Meloidae)

Alberto Sánchez-Vialas[1,2], Arnau Calatayud-Mascarell[3], José L. Ruiz[4], Ernesto Recuero[1,5], Mario García-París[1]

1 *Museo Nacional de Ciencias Naturales (MNCN-CSIC), c/ José Gutiérrez Abascal 2, 28006, Madrid, Spain*

2 *Instituto Madrileño de Investigación y Desarrollo Rural, Agrario y Alimentario (IMIDRA), Finca El Encín, Carretera A-2, km 38.2, Alcalá de Henares, 28805 Madrid, Spain*

3 *University of Idaho, Entomology, Plant Pathology and Nematology Department, 875 Perimeter Drive, MS 2329, Moscow, Idaho 83844-2329, USA*

4 *Instituto de Estudios Ceutíes, Paseo del Revellín 30, 51001, Ceuta, Spain*

5 *Department of Plant & Environmental Sciences, Clemson University, Clemson, South Carolina, USA*

https://zoobank.org/16CD6FE6-DFF6-43B2-8FBB-38E5A78B3704

Corresponding author: Alberto Sánchez-Vialas (alberto.alytes@gmail.com)

Received 16 June 2025
Accepted 25 October 2025
Published 26 February 2026

Academic Editors Vinicius S. Ferreira, Klaus-Dieter Klass

Citation: Sánchez-Vialas A, Calatayud-Mascarell A, Ruiz JL, Recuero E, García-París M (2026) Secondary sexual traits and lineage diversification in the giant blister beetle *Berberomeloe insignis* (Coleoptera: Meloidae). Arthropod Systematics & Phylogeny 84: 175–203. https://doi.org/10.3897/asp.84.e162254

Abstract

The evolutionary dynamics of morphological traits can often blur the boundaries between interspecific divergence and intraspecific variability, complicating species recognition. This study investigates the variation in secondary sexual traits and the existence of potential speciation processes within what is now considered *Berberomeloe insignis* (Coleoptera: Meloidae), an endangered blister beetle taxon endemic to southeastern Spain. Despite previous evidence of substantial genetic and phenotypic differentiation, key characters as the morphological variation in secondary sexual traits, such as antennomeres, remain unexplored. Using geometric morphometrics, we analyzed the shape variation of male and female antennomeres VII–XI across all previously recognized lineages of *B. insignis*. Our results reveal significant morphological differentiation, particularly in antennomeres VII, IX, and XI, which correlate broadly with genetic lineages. Based on the study of newly recorded populations, we confirm that cephalic coloration patterns correspond with mitochondrial lineages, further supporting the existence of geographic lineage differentiation within what was previously considered *B. insignis*. Climatic niche modeling indicates low climatic niche overlap between the isolated western lineage and the remaining lineages, which also show relatively low to moderate overlap, suggesting that ecological factors could have contributed to the divergence among them. These findings underscore the intricate interplay of genetics and ecology, highlight-ing the importance of integrating multiple data sources for accurate species delimitation. Based on our results, we describe *B. nazari* **sp. nov.** and *B. insignis trisanguinatus* **ssp. nov.** reflecting the evolutionary history of this group.

Keywords

geometric morphometrics, morphology, sexual dimorphism, taxonomy, endemism, Iberian Peninsula, new taxa

1. Introduction

Morphological diversification has often been associated with lineage isolation (Richards and Knowles 2007), although the strength and generality of this relationship remain debated (López-Estrada et al. 2025). Likewise, reduced time since divergence is frequently linked to limited phenotypic differentiation (Postma and van Noordwijk 2005), even if the tempo and mode of morphological evolution are far from uniform across lineages. Some deeply divergent species exhibit no obvious morphological differences (Pérez-Ponce de Leon and Poulin 2016; González-Miguéns et al. 2020), while others show marked intraspecific morphological variation (Kawano 2003; Pfenning and Pfenning 2010; Cuesta-Segura et al. 2023). At the same time, hybridization, following secondary contact among incipient species, can blur or homogenize these differences, limiting the ability to interpret genetic and morphological patterns of divergence (Taylor et al. 2006; Seehausen et al. 2008). In this context, a robust phylogenetic-phylogeographic framework is essential to fully understand how morphological traits evolve. Such a holistic approach can unravel the complexities of species differentiation (Pfennig and Murphy 2000; Richards and Knowles 2007; Darwell and Cook 2017; Moritz et al. 2017; Poso-Terranova and Andrés 2018; Cuesta-Segura et al. 2023), which is crucial for species delimitation by identifying genetic and morphological discontinuities across geographic ranges (Padial et al. 2010; Reyes-Velasco 2024).

Lineages inhabiting the southern European Mediterranean Peninsulas have gained significant attention for their remarkable genetic and morphological diversity, observed at both inter- and intraspecific levels. This diversity often follows the pattern of "southern richness and northern purity" (Hewitt 2000). Within the Iberian Peninsula, this pattern is evident in various taxa, where species richness is notably higher in the South compared to the North (Sánchez-Piñero 2006; Sánchez-Vialas et al. 2020). This phenomenon is also reflected at intraspecific levels, with southern populations often retaining ancient genetic and morphological traits lost in northern regions (Hewitt 2000). In this regard, northern populations are frequently recolonized from southern refugia, leading to the expansion of morphologically uniform traits due to founder effects (Hewitt 1996; Rodríguez-Flores et al. 2017). Consequently, organisms with limited dispersal abilities tend to exhibit greater inter- and intra-specific diversity in the southern regions of the Palaearctic.

One example of this pattern is represented by the genus *Berberomeloe* Bologna, 1988 (Coleoptera: Meloidae), a group of giant blister beetles following the "southern richness" pattern in the Iberian Peninsula. Due to its large size, diurnal activity, conspicuous coloration, and pharmacological properties, *Berberomeloe* is particularly popular in rural areas of Spain (see Percino-Daniel et al. 2013). Although familiar to local communities and entomologists for centuries, over half of the species in this genus have only recently been recognized (Sánchez-Vialas et al. 2020; Wrzecionko 2023). The genus is currently divided into two main species groups: the *B. majalis* (Linnaeus, 1758) and the *B. insignis* (Charpentier, 1818) species groups.

Southeastern Spain, from eastern Málaga to southeastern Alicante, is the most species-rich area for *Berberomeloe*, including six parapatric (and in some cases sympatric; García-París et al. 1999) species: *B. insignis*, *B. tenebrosus* Sánchez-Vialas, García-París, Ruiz & Recuero, 2020, *B. indalo* Sánchez-Vialas, García-París, Ruiz & Recuero, 2020, *B. majalis*, *B. payoyo* Sánchez-Vialas, García-París, Ruiz & Recuero, 2020, and *B. bubeniki* Wrzecionko, 2023. The first two species belong to the *B. insignis* species group, while the others fall within the *B. majalis* species group (Sánchez-Vialas et al. 2020; Wrzecionko 2023). A recent study revealed significant phylogeographic structure within *B. insignis*, a species endemic to southeastern Spain, with known populations across Murcia, Almería, and Granada (Sánchez-Vialas et al. 2023). The study identified four mitochondrial lineages, divided into two main clades approximately 2.1 million years old.

Currently, the four main mitochondrial lineages of *B. insignis* are known to be diagnosable only by cephalic coloration, as no other morphological differences have been identified (Sánchez-Vialas et al. 2023). Although the male antennal shape is diagnostic for some species of *Berberomeloe* (Sánchez-Vialas et al. 2020), the extent of variation in this secondary sexual trait within *B. insignis* remains unexplored.

Secondary sexual traits in insects, such as male-specific morphology, often evolve rapidly due to sexual selection, potentially contributing to reproductive isolation and aiding species delimitation (Eberhard 1985; True et al. 1997). In *Berberomeloe*, the shape of the last abdominal ventrite and antennomeres are well-known sexually dimorphic traits (Bologna 1991; García-París 1998; Sánchez-Vialas et al. 2020). For instance, the male antennae of *B. insignis* are characterized by strongly dentate antennomeres V, VII, and IX, distinguishing them from other congeneric species. Given the genetic and phenotypic divergence within *B. insignis* (Sánchez-Vialas et al. 2023), it is plausible that hidden morphological differences in secondary sexual traits may exist.

Based on the published molecular results by Sánchez-Vialas et al. (2023), this study aims to investigate the morphological diversity of secondary sexual traits in *B. insignis*, focusing on potential morphological discontinuities across the main known lineages. Since *Berberomeloe insignis* sensu lato is considered a threatened species categorized as "vulnerable" (García-París and Ruiz 2008, 2011; Sánchez-Vialas et al. 2023), and due to the interest from a conservation point of view, we also aim to confirm the lineage identity of several specimens from five newly recorded populations: Escúllar (Sierra de los Filabres) and Felix (Sierra de Gádor) in the province of Almería, Río de la Miel (Sierra de la Almijara) and Torre de Maro in province of Málaga, and Jete (between Sierra de los Guájares and Sierra de la Almijara) in province of Granada.

Table 1. Specimens used for molecular analyses. Locality, voucher number, and GenBank accession codes are provided.

Species of *Berberomeloe*	Locality in Spain	Voucher/catalog number	GenBank#CoxI	GenBank#16S
B. insignis trisanguinatus	Almería: Escúllar	ASV2402/MNCN_Ent 429909	PV034824	
B. insignis trisanguinatus	Almería: El Puntal	BiMAB181/ MNCN_Ent 325382	KC853087	KC853066
B. insignis trisanguinatus	Almería: El Puntal	BiMAB184/ MNCN_Ent 325383	KC853088	KC853067
B. insignis trisanguinatus	Almería: El Puntal	BiMAB193/-	MN252816	MN252646
B. insignis trisanguinatus	Almería: El Puntal	BiMAB194/-	MN252817	MN252647
B. insignis trisanguinatus	Almería: El Puntal	BiMAB195/-	MN252818	MN252648
B. insignis trisanguinatus	Almería: El Puntal	BiMAB196/-	MN252819	MN252649
B. insignis trisanguinatus	Almería: Peñas Negras-Los Perales	BiMAB192/ MNCN_Ent 325384	MN252815	MN252645
B. insignis trisanguinatus	Almería: 4.5 km south of Zurgena	BiMAB182/ MNCN_Ent 325385	KC853086	KC853065
B. insignis trisanguinatus	Almería: Tabernas	ASV18010/ MNCN_Ent 325386	OQ151517	OQ151611
B. insignis trisanguinatus	Almería: Tabernas	ASV19009/ MNCN_Ent 325387	OQ151521	OQ151615
B. insignis trisanguinatus	Almería: Tabernas	ASV19010/ MNCN_Ent 325388	OQ151522	OQ151616
B. insignis insignis	Murcia: Las Palas	ASV18023/ MNCN_Ent 325396		OQ151620
B. insignis insignis	Murcia: Mazarrón	ASV18040/ MNCN_Ent 325397	OQ151527	OQ151621
B. insignis insignis	Murcia: Morata	ASV18013/ MNCN_Ent 325398	OQ151520	OQ151614
B. insignis insignis	Murcia: Águilas	ASV18014/MNCN_Ent 429879	OQ151526	
B. nazari	Granada: La Garnatilla	ASV18041/MNCN_Ent 429968	OQ151523	OQ151617
B. nazari	Granada: La Garnatilla	ASV18042/MNCN_Ent 429969	OQ151524	OQ151618
B. nazari	Granada: La Garnatilla	ASV18043/MNCN_Ent 429970	OQ151525	OQ151619
B. nazari	Granada: Polopos	ASV18009/MNCN_Ent 429971	OQ151516	OQ151610
B. nazari	Granada: Jete	ASV21001/MNCN_Ent 429976	PV034818	PV034800
B. nazari	Granada: Jete	ASV21002/MNCN_Ent 429975	PV034819	PV034801
B. nazari	Granada: Jete	ASV21003/MNCN_Ent 429973	PV034820	PV034802
B. nazari	Granada: Jete	ASV21004/MNCN_Ent 429974	PV034817	PV034799
B. nazari	Málaga: Río de la Miel	ASV21008/MNCN_Ent 429964	PV034822	PV034804
B. nazari	Málaga: Torre de Maro	ASV21006/MNCN_Ent 429963	PV034821	PV034803
B. nazari	Málaga: Río de la Miel	ASV2201/MNCN_Ent 429966	PV034815	PV034797
B. nazari	Málaga: Río de la Miel	ASV2202/MNCN_Ent 429967	PV034816	PV034798
B. lineage C2	Almería: El Sabinar	ASV18011/MNCN_Ent 429949	OQ151518	OQ151612
B. lineage C2	Almería: Las Marinas	ASV18012/MNCN_Ent 429948	OQ151519	OQ151613
B. lineage C2	Almería: Felix	ASV2401/MNCN_Ent 429911	PV034823	

We hypothesize that (1) molecular divergence and morphological differentiation in secondary sexual traits would change at the same rate, potentially indicating completed speciation, and (2) hybridization between lineages in *Berberomeloe* may limit morphological divergence, leading to the formation of intermediate phenotypes. Given the threats that *Berberomeloe* faces due to habitat destruction and vulnerability to greenhouse expansions (Sánchez-Vialas et al. 2023), precise taxonomic identification at species and subspecies levels is crucial and critical for effective conservation efforts (Dufresnes et al. 2023).

2. Material and methods

2.1. DNA extraction, sequencing, and phylogenetic analyses

To confirm the molecular identification of the five newly recorded populations (Escúllar, Felix, Torre de Maro, Río de la Miel, and Jete), we sequenced one to four specimens from each locality (Table 1). Mitochondrial gene fragments of the cytochrome oxidase subunit I (*CoxI*) and 16S ribosomal RNA (*16S*) were targeted for this purpose.

Genomic DNA was extracted from femoral muscular tissue using the Qiagen DNeasy extraction kit (Qiagen, Valencia, CA, USA). Polymerase chain reaction (PCR) was used to amplify *CoxI* and *16S* using the set of primers LCO 1490/COI-H (Folmer et al. 1994; Machordom et al. 2003) and 16Sar/16Sbr (Palumbi et al. 1991), respectively. PCR conditions followed those described in Sánchez-Vialas et al. (2020). The PCR products were sequenced in both directions by Sanger Sequencing at Macrogen (Madrid, Spain).

Sequences were reviewed, assembled, and edited in Geneious v.11.0.18 and aligned using MAFFT (Katoh and Toh 2008). Phylogenetic analyses were conducted in BEAST v.1.10.4, following the dataset and methodology of Sánchez-Vialas et al. (2023), with the three newly generated sequences into the analysis incorporated.

Additionally, a phylogenetic network was generated using SplitsTree v.6.3.41 (Huson and Bryant 2006) based on combined *CoxI* and *16S* mitochondrial sequences for all specimens possessing both markers. Although

these markers reflect the maternal lineage, the network approach helps identify conflicting signals in the data – such as incomplete lineage sorting or historical gene flow – that may not be evident in traditional tree-based analyses. This method is particularly useful for detecting conflicting signals that might be obscured in traditional phylogenetic trees, offering a more comprehensive view of the evolutionary history.

We also considered the nuclear ITS2 allele data from Sánchez-Vialas et al. (2023) as additional evidence to support taxonomic decisions.

2.2. Genetic distances and isolation by distance

To investigate a possible effect of isolation by distance (IBD) within *B. insignis* sensu lato, we used the *CoxI* dataset to derive a genetic distance matrix (Table S1) using MEGA X (Kumar et al. 2018). We selected *CoxI* because it is the most comprehensively represented gene in our matrix, shared by all sequenced specimens except one (N = 30). Genetic distance matrices were calculated using uncorrected genetic distances.

Geographic distances were calculated from georeferenced locality data (Table 1), obtained using Google Earth Pro. These distances were converted to Euclidean distances in kilometers using the distHaversine function from the geosphere package (Hijmans et al. 2017).

To assess the correlation between geographic and genetic distances, we conducted Mantel tests using the mantel function from the R package Vegan (Oksanen et al. 2013). Analyses were performed separately for each matrix, with results visualized through scatterplots.

2.3. Morphological study

A total of 182 specimens were examined, including 168 housed at the Museo Nacional de Ciencias Naturales (MNCN-CSIC, Madrid, Spain) and 14 at the Museo de Ciencias Naturales de Tenerife (MUNA, Sta. Cruz de Tenerife, Spain). Of these, 126 specimens were preserved in ethanol, while 56 were dry-preserved (Table S2). Additionally, detailed photographs of the holotype (by monotypy) of *Meloe insignis* Charpentier, 1818, deposited at the Museum für Naturkunde-Berlin (MNB, Berlin, Germany), were examined. These images were kindly provided by Bernd Jaeger, curator of Coleoptera at MNB. The holotype of *Meloe insignis* is labeled as follows: "Hist.-Coll. (Coleoptera), Nr.28477, *Meloe insignis* Charp., Zool. Mus. Berlin [with label, printed]; insignis, 1798. Typ. Charp* [white label, handwritten]; Type [red label, printed]; [QR code with former MFN collection URI].

Ethanol-preserved and dry-mounted specimens were examined under a stereomicroscope. Selected male specimens were rehydrated in water prior to genitalia extraction. For dry-mounted specimens, male genitalia were mounted on a cardboard using dimethylhydantoin formaldehyde (DMHF) resin and pinned adjacent the specimen. In ethanol-preserved specimens, male genitalia were stored in an Eppendorf tube filled with 96% ethanol, kept within the vial of the specimen. Measurements were taken from images captured using a Leica MZ16A

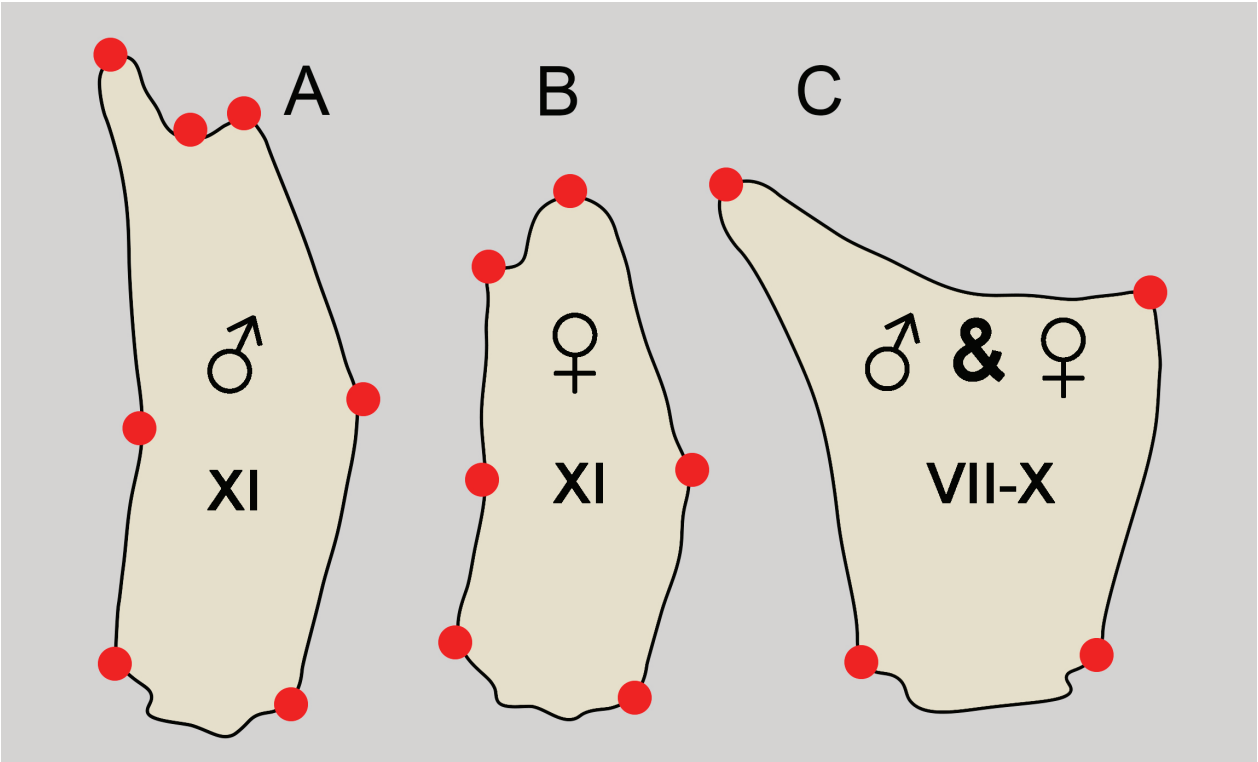

Figure 1. Landmarks (red dots) used for *Berberomeloe* antennomeres in this study. Landmarks on male (**A**) and female (**B**) antennomere XI. Landmarks on antennomeres VII, VIII, IX, and X, for both sexes (**C**).

stereomicroscope, fitted with a Leica DFC550 camera and processed with the software LAS v.4.3. Terminology for the male genitalia follows Selander (1966).

We conducted geometric morphometric analyses (GM) focusing on the shape variation of the last five antennomeres (VII–XI) in relation to four mitochondrial lineages of *Berberomeloe insignis* identified by Sánchez-Vialas et al. (2023): B1 (Murcia), B2 (eastern-central Almería), C1 (Granada), and C2 (south-central Almería). Male and female antennomeres were analyzed; antennomeres VII, IX, and XI showed sexual dimorphism, while antennomeres VIII and X did not. The analysis was based on 92 adult specimens, preserved dried or in ethanol. Among these, 55 were males, distributed across lineages B1 (13 specimens), B2 (15 specimens), C1 (13 specimens), and C2 (14 specimens), and 37 were females, distributed across lineages B1 (7 specimens), B2 (8 specimens), C1 (13 specimens), and C2 (9 specimens) (Table S3). Digital images of the inner side of left antennae (or right antenna, if left absent) were captured using a reflex camera coupled with a macro lens, mounted on a stable camera stand. For antennomeres VII–X, four anatomical landmarks were used, while for antennomere XI, seven anatomical landmarks were used for males and six for females (Fig. 1). Landmarks were digitized using the R package "StereoMorph" v.1.6.2. (Olsen and Westneat 2015) within R v.3.6.0 (R Core Team 2021). The coordinates (X, Y) obtained from landmark digitization were subjected to generalized Procrustes analyses (Gower 1975) to normalize for differences in position, orientation, and scale. Mean shapes were then computed for each lineage, and principal component analysis (PCA) was performed on these shapes. PCA was conducted on the coordinates projected into the linear tangent space using the function gm.prcomp. The first two principal components were used to visualize the variation in antennomere shape. Procrustes ANOVA with 1000 permutations was used to assess significant differences between clades.

2.4. Distribution data collection

Geographic records of *B. insignis* were compiled from previously published data (mainly García-París 1998; García-París et al. 1999, 2003; García-París and Ruiz 2008, 2011; Sánchez-Vialas et al. 2023), unpublished records from fieldwork (samplings carried out by the authors in the last five years), and observations taken from iNaturalist (www.inaturalist.org) (Table S4). From iNaturalist records, only those with high accuracy (N = 37) were used, excluding those with coordinate errors exceeding 1 km. Each iNaturalist observation was carefully assigned to its corresponding taxonomic unit based on cephalic coloration patterns.

2.5. Niche modeling-overlap

The potential geographic distribution ranges of the five different lineages of *Berberomeloe insignis* were inferred using MaxEnt 3.4.1 (Phillips et al. 2017). MaxEnt estimates the interaction between environmental variables and species presence to create suitability models for a geographic area. Analyses were based on all known localities (Table S4). Nineteen bioclimatic layers were retrieved from the WorldClim 2.1 database (www.worldclim.org) at a 30 second resolution (Fick and Hijmans 2017). To avoid collinearity among predictors, we performed a Pearson correlation analysis in R using the package 'corrgram' (Wright 2006). When two variable showed a correlation coefficient higher than 0.8, only the one considered biologically more relevant for the species was retained. Based on this criterion, the following subset was selected: bio7 – Temperature Annual Range, bio8 – Mean Temperature of Wettest Quarter, bio11 – Mean Temperature of Coldest Quarter, bio14 – Precipitation of Driest Month, bio15 – Precipitation Seasonality (Coefficient of Variation), bio16 – Precipitation of Wettest Quarter. Analyses in MaxEnt were conducted using the cross-validation testing procedure recommended for small datasets (Philips et al. 2006). The MaxEnt output was set to Cloglog, which estimates the probability of presence between 0 and 1. The outputs were further edited with QGIS 3.22 Białowieża (www.qgis.org) to generate distribution maps.

Potential ecological interchangeability among the different lineages within the two main clades was evaluated by measuring niche overlap using Schoener's D-metrics (Wooten and Gibbs 2012). Pairwise comparisons were conducted, and niche identity tests were performed using 100 randomized pseudoreplicates to determine if the Schoener's D-values were statistically different (one-tailed test) than expected under the null distribution. Niche conservatism or divergence was inferred by comparing the niche overlap values with the null distribution of overlap values. Niche divergence is supported when the overlap values are smaller than the null distribution. These analyses were conducted with the R package "ENMTools" (Warren et al. 2021).

2.6. Species concept and delimitation

Distinguishing between interspecific and intraspecific variation is a challenging task (Pyron et al. 2020, 2024). To address species delimitation, we adopted the general lineage (unified) species concept (de Queiroz 1998, 2007), which considers a species as "separately evolving metapopulation lineages". Based on this framework, we recognize species when populations show consistent patterns in both mitochondrial and nuclear DNA sequences (as demonstrated by the nuclear allelic network of ITS2 in Sánchez-Vialas et al. 2023) and exhibit concordant morphological traits. These multiple lines of evidence suggest that the lineages in question are evolving independently and have achieved reproductive isolation with minimal likelihood of future interbreeding, especially when the lineages involved are parapatric or sympatric.

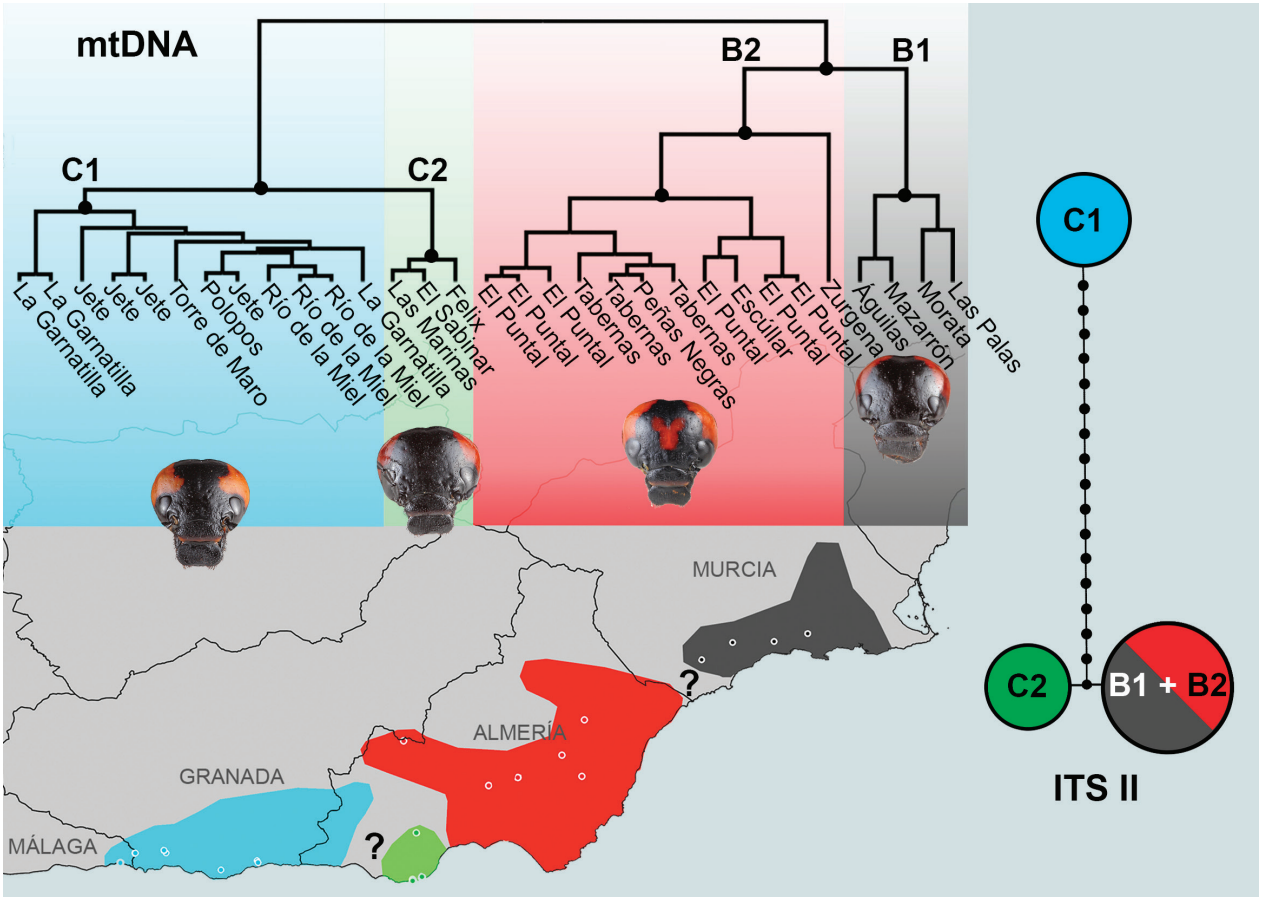

Figure 2. Phylogenetic relationships and geographic distribution of *Berberomeloe insignis* sensu lato. The mitochondrial phylogenetic tree (*Cox1* and *16S*) and the ITS2 allelic network (adapted from Sánchez-Vialas et al. 2023) are shown. The map illustrates the geographic range of each major clade, with distinct colors matching those in the phylogeny and allelic network. Cephalic phenotypes for each clade are also depicted. Clade labelling follows Sánchez-Vialas et al. (2023). Nodal support of PP > 90 is indicated by a dot.

3. Results

3.1. Molecular phylogenetic analysis and phylogenetic networks

The newly generated *Cox1* (657 bp) and *16S* (510 bp) sequences have been deposited in GenBank (Table 1). We recovered the same topology for *Berberomeloe insignis* sensu lato as in Sánchez-Vialas et al. (2023). Each of the newly sampled populations corresponds with its respective phenotypically diagnosable lineages (Fig. 2). Following the clade denominations of Sánchez-Vialas et al. (2023), the sequenced specimen from Escúllar (Sierra de los Filabres) is nested within the mitochondrial DNA (mtDNA) clade B2, the specimen from Felix (Sierra de Gádor) belongs to clade C2, and those from Río de la Miel, Torre de Maro, and Jete belong to clade C1.

The phylogenetic network generated using SplitsTree revealed a well-defined and cohesive lineage (C) encompassing populations from Granada, Málaga (C1), and western Almería (C2). Within this lineage, the specimens from western Almería showed a relatively genetic differentiation from western areas (C1). The clade C is clearly separated from the others by a long branch, indicating limited interaction with other lineages. In contrast, the remaining clades (B) exhibited a more intricate pattern, with high genetic differentiation but multiple reticulations (nexus points) within the network, suggesting extensive historical gene flow among them (Fig. 3).

3.2. Isolation by distance

The Mantel test results revealed low correlation between geographic and genetic distances across populations of *Berberomeloe insignis* sensu lato. Although the correlation was statistically significant (Mantel statistic r = 0.1165, P = 0.033), it remained notably weak (Fig. 4). This suggests that genetic differences among lineages are not primarily driven by geographic distance.

3.3. Geometric morphometric analyses

GM analyses of male antennomeres revealed a complex pattern of morphological variation (Figs 5, 6). Anten-

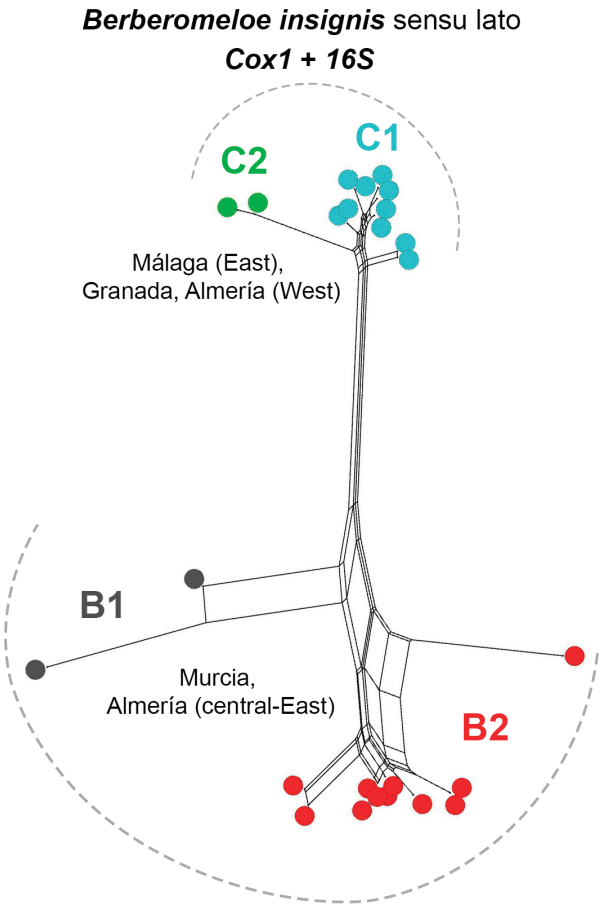

Figure 3. SplitsTree phylogenetic network for *Berberomeloe insignis* sensu lato.

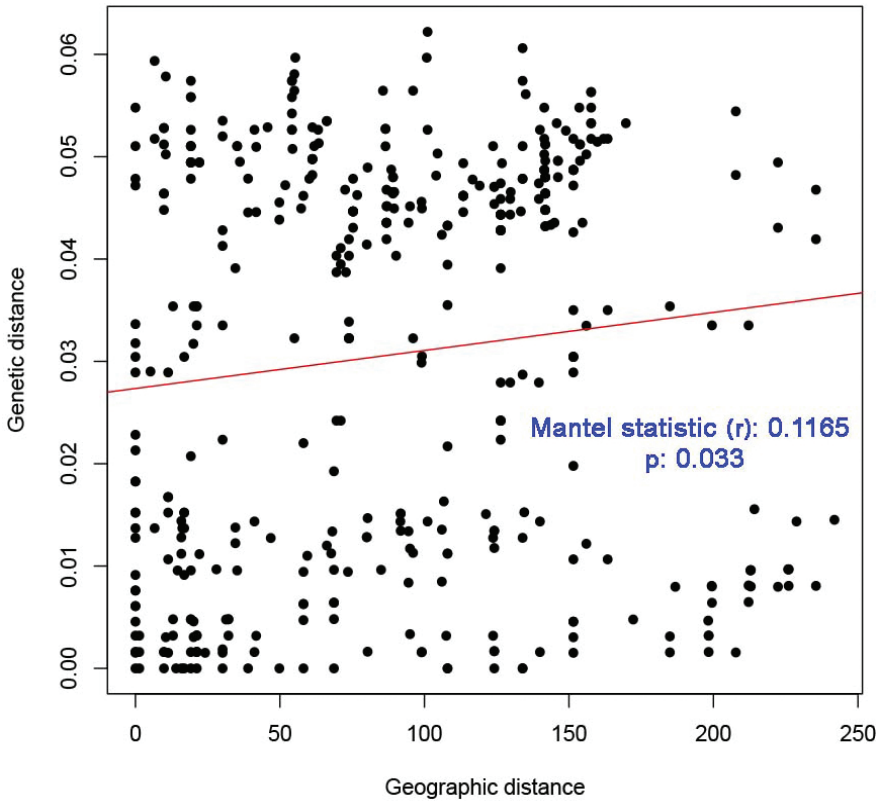

Figure 4. Isolation by distance plot among populations of *Berberomeloe insignis* sensu lato. The red line illustrates the correlation between geographic (in Km) and genetic distances. The Mantel statistic and its significance level are depicted in blue.

nomere XI exhibited significant differences across most clades (Table S5), with the exception of the lineages of Central-Eastern Almería and Campo de Dalías (lineages B2 and C1 respectively, sensu Sánchez-Vialas et al. 2023), which showed a considerable overlap (Fig. 5). Antennomere X displayed substantial overlap among most

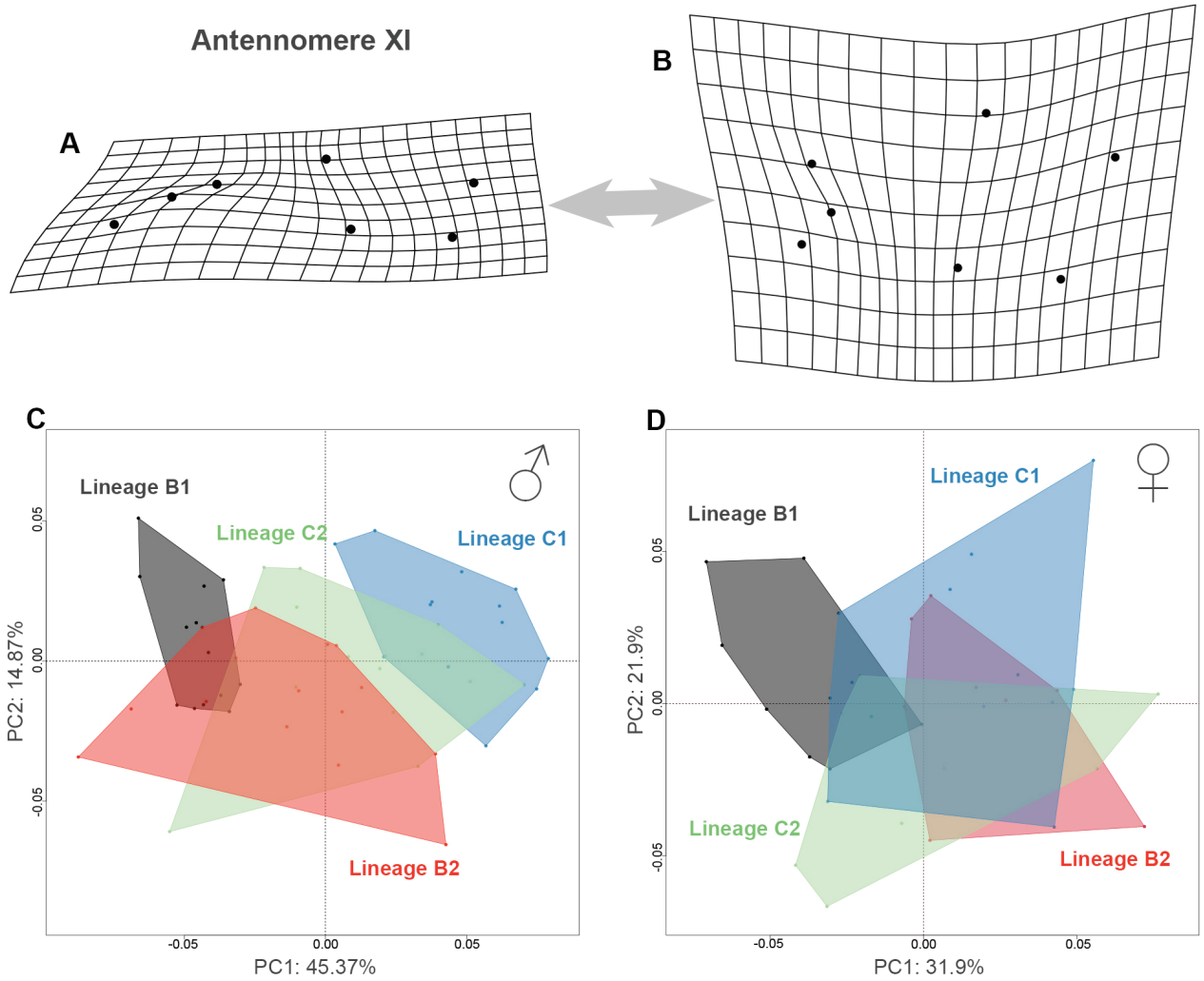

Figure 5. Deformation grids showing shape variation of *Berberomeloe* antennomere XI in males from Tabernas, lineage B2 (**A**) and Jete, lineage C1 (**B**). **C**, **D** Principal component analysis of antennomere XI for both sexes. Black polygon: mtDNA clade B1; red polygon: mtDNA clade B2; green polygon: mtDNA clade C2; blue polygon: mtDNA clade C1.

clades, except for the one from Murcia (lineage B1 sensu Sánchez-Vialas et al. 2023), which showed significant differentiation. Antennomere IX followed the pattern of antennomere XI, with strong differentiation among lineages from Málaga-Granada, Murcia, and Central-eastern Almería, but with considerable overlap between the Central-Eastern Almería and Campo de Dalías clades. Antennomere VIII distinguished the Murcia lineage but did not differentiate among the other clades. Antennomere VII displayed significant differentiation between the Málaga-Granada clade and other clades, with less pronounced differences between the Central-eastern Almería and Murcia clades ($P = 0.02$) and between the Central-eastern Almería and Campo de Dalías clades ($P = 0.04$) (Fig. 6).

In females, antennomeres showed substantial overlap among clades, except for the Murcia clade (B1), which exhibited clear differentiation from the others (Fig. 7). Notably, antennomere XI revealed a significant distinction between the C1 clade (Málaga-Granada) and the B2 clade (Central-Eastern Almería) (Table S4).

PCA for males indicated that PC1 and PC2 accounted for 45.37% and 14.87% of the variability for antennomere XI, 65.63% and 22.69% for antennomere X, 54.97% and 27.81% for antennomere IX, 67.65% and 19.75% for antennomere VIII, and 46.18% and 26.13% for antennomere VII. For females, PC1 and PC2 explained 31.9% and 21.9% of the variability for antennomere XI, 77.44% and 11.19% for antennomere X, 72.37% and 14.89% for antennomere IX, 66.16% and 18.66% for antennomere VIII, and 62.87% and 20.11% for antennomere VII.

In summary, all major clades (B1, B2, C1) can be distinguished based on variation in antennomeres, with the exception of the potentially hybrid populations represented by the mitochondrial subclade C2 (Campo de Dalías and southern Sierra de Gádor), which consistently exhibit significant overlap with other clades.

3.4. Coloration patterns

Head coloration patterns of the newly reported specimens are geographically congruent with their corresponding mitochondrial lineages (Sánchez-Vialas et al. 2023). Populations from Málaga, Granada, and the southwestern edge of Almería (clade C1 of Sánchez-Vialas et al. 2023) displayed two symmetrical red-orange blotches on the tem-

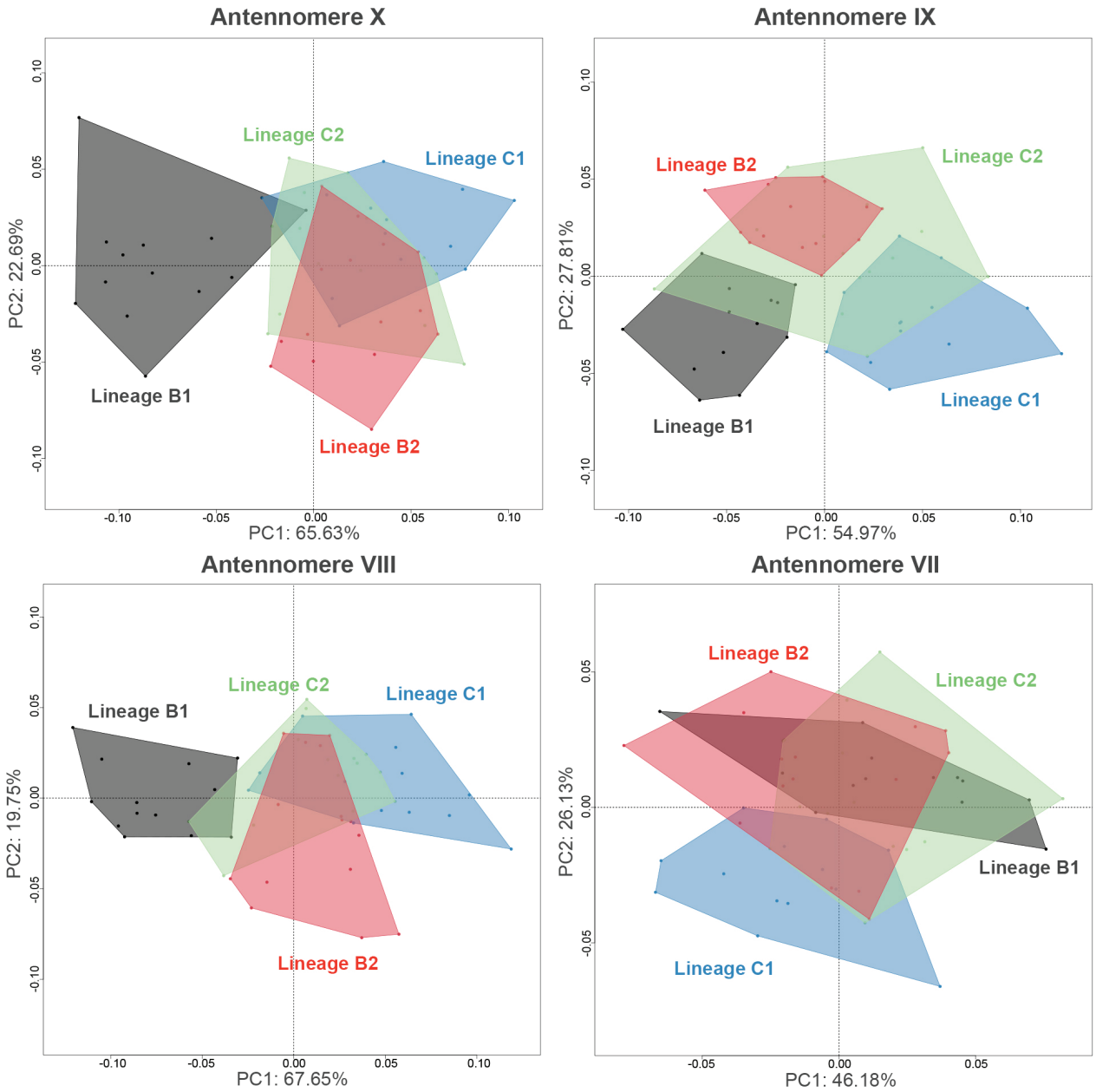

Figure 6. Principal component analysis of *Berberomeloe* male antennomeres VII, VIII, IX, and X. Black polygon: mtDNA clade B1; red polygon: mtDNA clade B2; green polygon: mtDNA clade C2; blue polygon: mtDNA clade C1.

ples, slightly extending toward the frons (but not reaching the frons midline). Eastern Almería and Pasillo de Fiñana Valley (between Sierra Nevada and Sierra de los Filabres) populations (clade B2 of Sánchez-Vialas et al. 2023) exhibited three blotches: two symmetrical ones over the temples that do not extend towards the frons and a central V- or Y-shaped blotch on the frons. The Murcia phenotype (clade B1 of Sánchez-Vialas et al. 2023) resembles that from B2 but lack the central blotch on the frons. The remaining phenotype, located in Campo de Dalías and the southern slope of Sierra de Gádor (clade C2 of Sánchez-Vialas et al. 2023), resembles B1 but with wider separation of the temporal blotches at the occiput. Occasional, inconspicuous red blotches (very small and circular on both sides of the frontal midline, either isolated or connected to the temporal blotches) were also observed in some specimens from the southern areas of Sierra de Gádor.

3.5. Climate niche modeling-overlap

The species distribution models (SDMs) performed well for the lineages of *B. insignis*, as indicated by high Area Under the Curve (AUC) values: Murcia (clade B1): AUC = 0.962; Eastern Almería and Pasillo de Fiñana Valley (clade B2): AUC = 0.950; Málaga, Granada, and the southwestern edge of Almería (clade C1): AUC = 0.983; Campo de Dalías and southern Sierra de Gádor (clade C2): AUC = 0.985. In addition, the SDM for all main lineages of *B. insignis* sensu lato yielded an AUC of 0.926.

The environmental variables that contributed most to the models varied by clade: for clade B1, bio16 (51.4%) and bio14 (15.9%); for clade B2, bio16 (50.2%) and bio15 (30.5%); for clade C1, bio6 (50.6%) and bio7 (25.3%); and for clade C2, bio14 (30.9%) and

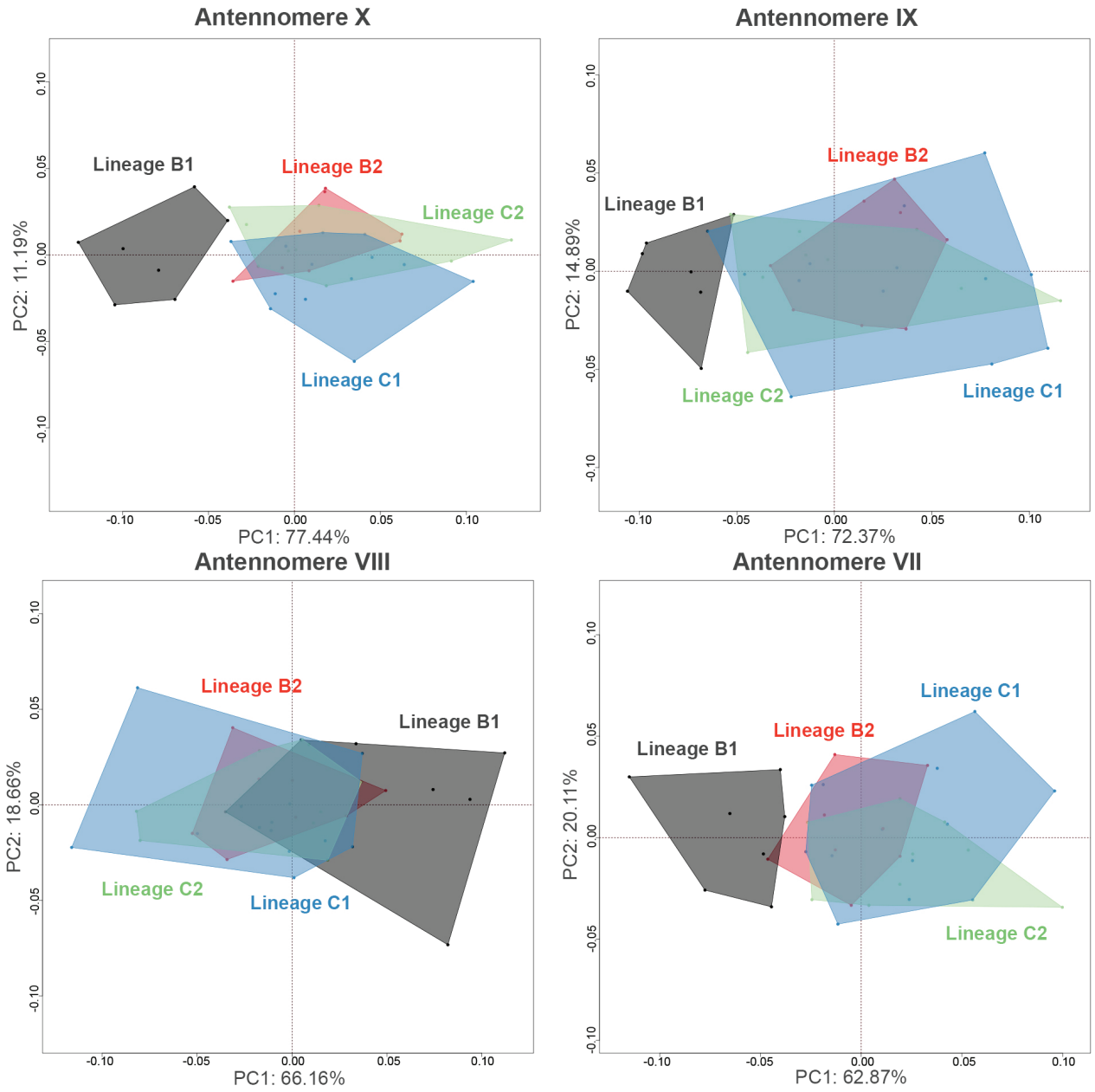

Figure 7. Principal component analysis of *Berberomeloe* female antennomeres VII, VIII, IX, and X. Black polygon: mtDNA clade B1; red polygon: mtDNA clade B2; green polygon: mtDNA clade C2; blue polygon: mtDNA clade C1.

bio7 (30.4%). Across all lineages of *B. insignis*, bio16 (61.3%) and bio15 (14%) were the primary contributing variables.

Niche overlap, measured using Schoener's D-metric, was low between clade C1 (Málaga, Granada, and the southwestern edge of Almería) and other clades, and relatively low to moderate among the different clades of *B. insignis* sensu lato (Table 2). All comparisons were statistically significant, indicating that the lineages are not ecologically interchangeable (Figs S1–S6).

3.6. Taxonomic output

Sánchez-Vialas et al. (2023) highlighted strong genetic isolation between the westernmost lineage (C1) and the other lineages, supported by nuclear and mitochondrial DNA. Considering this criterion, the morphological differences among the main units within *B. insignis*, and the species concept adopted (see material and methods), we propose recognizing two distinct species within the current conception of *B. insignis* sensu lato: one comprising lineage C1, which ranges from eastern limit of Málaga province (new faunistic records), southern Granada, and western limit of Almería province; and a second species comprising two subspecies distributed across Murcia (lineage B1) and eastern Almería (lineage B2).

According to this new taxonomic framework, since *B. insignis* sensu lato includes two candidate species, it is necessary to assign the original name to one of the two species. Charpentier (1818: 258) described *Meloe insignis* from Spain (type locality: "Spanien") without pre-

Figure 8. Holotype of *Meloe insignis* (currently *Berberomeloe insignis*). Original drawing of the type specimen from Charpentier's (1818) description, sourced from the Biodiversity Heritage Library (https://www.biodiversitylibrary.org) (**A**). Frontal (**B**) and dorsal (**C**) views of the type of *B. insignis* housed at the Museum für Naturkunde Berlin, with labels shown in (**C**). Photographs: Ivo Jurisch, Museum für Naturkunde Berlin.

cise locality. From the original description it can be concluded without any doubt that the species was described based on a single specimen, which constitutes the holotype fixed by monotypy (art. 73.1.3 of the International Code of Zoological Nomenclature; ICZN 1999). The type specimen illustrated in the original description shows a diagnostic head coloration pattern: two symmetric, reddish blotches on the temples, close to each other at the occiput, with no frontal blotch (Fig. 8A), confirmed by examining detailed photographs of the holotype (Fig. 8B, C). Thus, the phenotype of the name-bearing type (holotype) is characteristic and exclusive of the populations of Murcia province, corresponding to the B1 lineage. Therefore, we assign the name *Berberomeloe insignis* (= *Meloe insignis*) to B1 lineage populations. As no synonyms exist for *B. insignis*, the new species (C1) and subspecies (B2) recognized here require, in turn, new names.

However, the situation becomes more complex for the populations of the lineage C2. Historical genetic introgression appears to explain the observed cyto-nuclear discordance in the populations from southwestern Almería (lineage C2). While mitochondrial DNA places these populations closer to the westernmost lineage (C1), nuclear ITS2 data aligns them more closely with the central-eastern Almería and Murcia populations (lineage B). Although geographically restricted to a small area in southern Almería, specimens from lineage C2 exhibit broad morphological variation, overlapping with their parapatric lineages. C2 populations are nevertheless distinguishable by a singular head coloration (see Sánchez-Vialas et al. 2023: figs 13, 14), yet some specimens from the southern slopes of Sierra de Gádor exhibit variability that may reflect a legacy of past hybridization. However, the available molecular data are limited, with only a few C2 individuals genotyped for mitochondrial DNA and ITS2, and consequently a significant portion of genetic diversity in these populations remains uncharacterized. Given these uncertainties, together with the absence of any fully diagnostic morphological trait, there is currently insufficient evidence to assess the extent of reproductive isolation between lineage C2 and its parapatric species (see discussion).

The current taxonomic catalogue for *B. insignis* should be modified with the following descriptions and diagnosis:

Berberomeloe insignis (Charpentier, 1818)

Meloe insignis Charpentier in Germar, 1818: 258. Type locality: "Spanien"

Berberomeloe insignis (Charpentier, 1818): García-París, 1998: 99.

Berberomeloe insignis insignis (Charpentier, 1818)

Meloe insignis Charpentier in Germar, 1818: 258. Type locality: "Spanien"

Berberomeloe insignis (Charpentier, 1818): García-París, 1998: 99.

Description. Detailed descriptions of *B. insignis* s.l. were provided by García-París (1998) and Sánchez-Vialas et al. (2020). Currently, only the information derived from populations of *B. insignis* s.l. from Murcia refers to this subspecific taxon. This subspecies corresponds to the B1 lineage as defined by Sánchez-Vialas et al. (2023).

Diagnosis and comparisons. *Berberomeloe insignis insignis* can be differentiated from other taxa of the *B. insignis* species group by the presence of (1) two symmetric red- to orange-colored blotches over the temples that do not extend anteromedially as a lobate projection above the ocular margin; (2) absence of a V- or Y-shaped mark on the frons; (3) strongly elongated antennomeres in both sexes; (4) elongated male genitalia (Fig. 9).

From *B. insignis trisanguinatus* **ssp. nov.** (B2 lineage) it can be readily differentiated by the lack of the red V- or Y-shaped mark on the frons, different shape of male antennomeres VII–XI and more elongated female antennomeres VII–XI. From *B. nazari* **sp. nov.** it differs by a

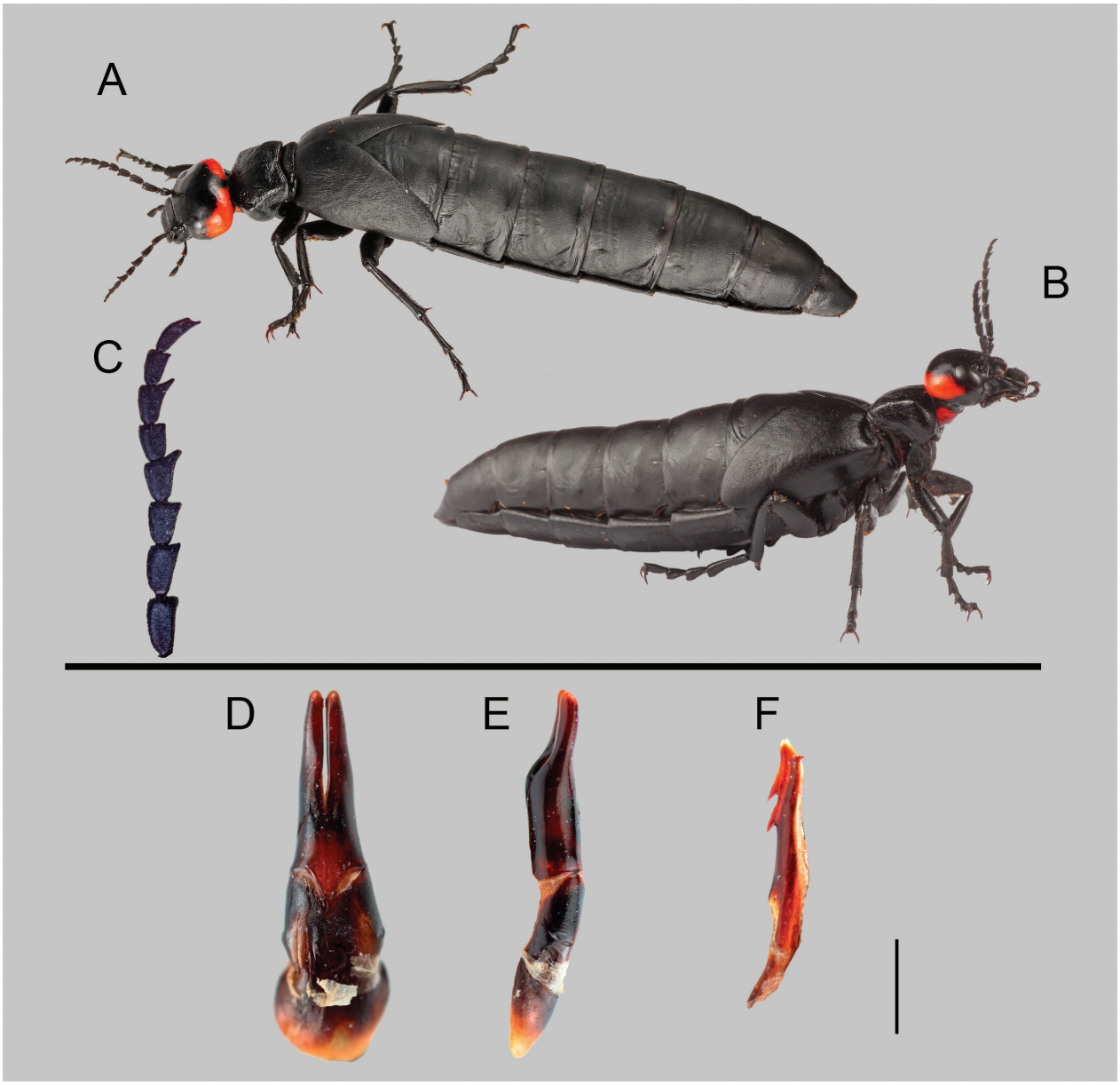

Figure 9. *Berberomeloe insignis insignis*. Male from Mazarrón, Murcia (**A**). Male from las Palas, Murcia (**B**). Male antennomeres IV–XI from a specimen from Las Palas, Murcia (**C**). Male genitalia of specimen MNCN_Ent 429864 from 1.5 km northeast of Morata, Murcia (**D–F**): ventral and lateral views of the gonoforceps (**D**, **E**), and lateral view of the aedeagus (**F**); scale bar: 1 mm.

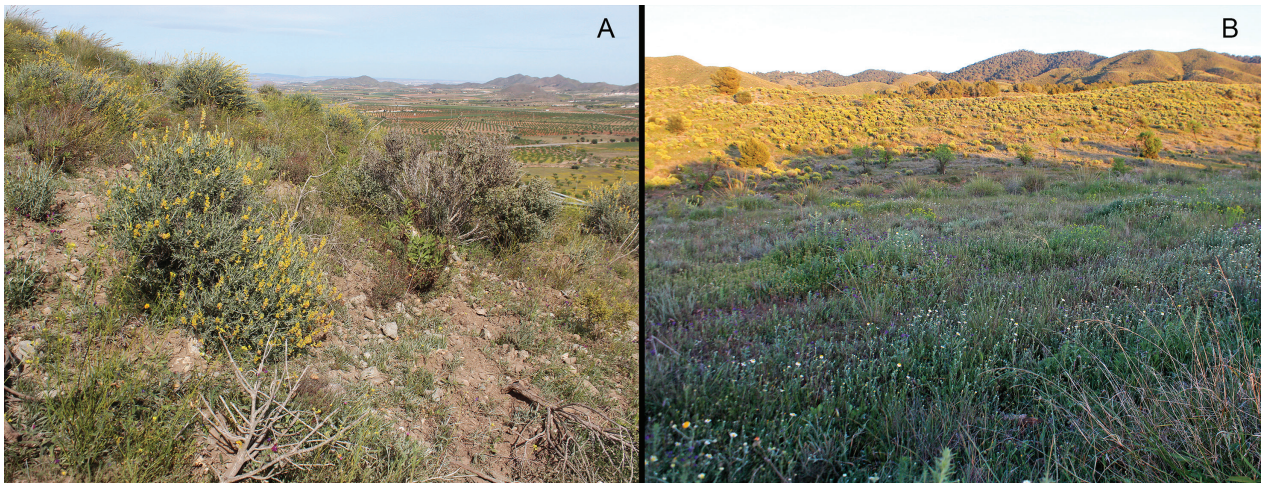

Figure 10. Habitats of *Berberomeloe insignis insignis*. Landscape between Las Palas and Mazarrón, Murcia (**A**). Surroundings of Ermita de Villareal, 18 km north of Águilas, Murcia (**B**).

more regular shape of the marks of the temples, that do not extend to the frons bordering the upper ocular margin area, by different shape of male antennomeres VII–XI, and by more elongated antennomeres VII–XI in female. The most phenotypically similar populations to *Berberomeloe insignis insignis* are those from Campo de Dalías and southern Sierra de Gádor (lineage C2) from which it can be distinguished by the closer proximity of the blotches on the temples in the occipital area, distinct shapes of male antennomeres VIII–XI, and by the more elongated antennomeres VII–XI in female (Table S5).

Variability. Females have the last exposed abdominal tergite VIII rounded, not emarginated at its posterior margin, with antennomeres IX, VII, and V less widened apically, and the last antennomere wider in its apical area.

Distribution and notes on natural history. According to the available distribution data, this subspecies is endemic to the province of Murcia, primarily inhabiting coastal and subcoastal areas from sea level to 630 m a.s.l.. Some populations extend inland up to 30 km from the coast, particularly around Sierra de Carrascoy (Majal Blanco) and South to the city of Murcia (Algezares) (García-París and Ruiz 2011; Table S4). Within this range, *B. insignis insignis* occupies xerothermic scrublands with sparse low vegetation (Fig. 10), such as *Ziziphus lotus* (L.) Lam., *Maytenus senegalensis* (Lam.) Excell, *Periploca angustifolia* Labill., *Pistacia lentiscus* L., *Chamaerops humilis* L., *Retama sphaerocarpa* (L.) Boiss., *Calicotome intermedia* C. Presl, *Launaea arborescens* (Batt.) Murb., *Anthyllis cytisoides* L., *Rhamnus lycioides* L., *Gypsophila struthium* Loefl., and *Macrochloa tenacissima* (L.) Kunth (see Alcaráz and Peinado 1987; Sánchez-Gómez et al. 1998; Valle 2003; Carrión et al. 2008). This habitat also supports biogeographically significant plant species, such as *Tetraclinis articulata* (Vahl) Masters, which is native to North Africa, Malta, and the Spanish province of Murcia (Esteve Selma et al. 2017), along with other species endemic to Murcia: *Limonium carthaginense* (Rouy) C.E. Hubb & Sandwith, *Teucrium carthaginense* Lange, *Astragalus nitidiflorus* Jiménez & Pau, and *Asparagus macrorrhizus* Pedrol. Adults of this subspecies have been observed feeding on flowers of *Convolvulus* L. and leaves of Asteraceae (authors pers. obs.).

We have revised the coordinates of "Algezares" as reported by Sánchez-Vialas et al. (2023). The correct location is not in the town of Algezares in the northern part of the province of Murcia, but rather in the neighborhood of Algezares, located south of the city of Murcia, near the Sierra de Carrascoy.

It has been found in sympatry with *Berberomeloe majalis* (Linnaeus, 1758) in the surroundings of Isla Plana (authors pers. obs.).

Berberomeloe insignis trisanguinatus Sánchez-Vialas, Calatayud-Mascarell, Ruiz, Recuero, and García-París ssp. nov. (B2 lineage)

https://zoobank.org/2937E761-EE8A-4378-9BC3-B19C7ACBF7BB

Type material. Holotype: Male, labeled: España, Escúllar, Almería, 37°10′51.4″N 2°44′31.6″W, 18-IV-2024, Sánchez Vialas, A. leg. [white label, printed]; MNCN_Ent 429880 [white label, printed]; Holotypus, *Berberomeloe insignis trisanguinatus* Sánchez-Vialas, Calatayud-Mascarell, Ruiz, Recuero & García-París des. 2025 [white label, printed]. Preserved in absolute ethanol at the Entomological collection of the Museo Nacional de Ciencias Naturales, Madrid. — **Paratypes** (29 exx, all held at the Entomological collection of the Museo Nacional de Ciencias Naturales, Madrid): 7 males and 14 females labeled: España, Almería, Tabernas, alrededores, 389 m, 37°05′43.04″N 02°05′15.07″W, 29-III-2008, E. Recuero and C. Settanni leg. [white label, printed]; BI264, 267, 270, 272, 277, 283, 284, 226, 263, 265, 268, 269, 273–276, 278–282 [white label, handwritten; 7 males and 14 females, respectively]; MNCN_Ent 429901, MNCN_Ent 429900, MNCN_Ent 429897, MNCN_Ent 429899, MNCN_Ent 429896, MNCN_Ent 429895, MNCN_Ent 429898, MNCN_Ent 429890, MNCN_Ent 429882, MNCN_Ent 429881, MNCN_Ent 429883, MNCN_Ent 429892, MNCN_Ent 429891, MNCN_Ent 429894, MNCN_Ent 429887,

MNCN_Ent 429889, MNCN_Ent 429886, MNCN_Ent 429884, MNCN_Ent 429888, MNCN_Ent 429885, MNCN_Ent 429893 (preserved in ethanol). – 1 male, labeled: España, Almería, 10 km E Tabernas, 489 m, 37°04′50.1″N 02°19′21.4″W, 28-III-2008, E. Recuero and C. Settanni leg. [white label, printed]; MNCN_Ent 429902 [white label, printed] (preserved in ethanol). – 6 females, labeled: España, Almería, Las Casillas de Atochares, 36°52′53.0″N 02°10′13.2″W, 30-III-2008, E. Recuero and C. Settanni leg. [white label, printed]; BI315–318, BI334–335 [white label, handwritten]; MNCN_Ent 429903–429908 [white label, printed] (females, preserved in ethanol). – 1 male, labeled: España, Almería, Escúllar, 37°10′51.4″N 2°44′31.6″W, 18-IV-2024, Sánchez Vialas, A. leg. [white label, printed]; ASV2402 [white label, handwritten]; MNCN_Ent 429909 [white label, printed] (preserved in ethanol). All paratypes labeled: Paratypus, *Berberomeloe insignis trisanguinatus* Sánchez-Vialas, Calatayud-Mascarell, Ruiz, Recuero & García-París des. 2025 [white label, printed].

Etymology. The specific epithet "*trisanguinatus*" is a Latin adjective meaning "three-blooded", referring to the species' distinctive cephalic phenotype. This taxon is unique within the genus *Berberomeloe* for its three conspicuous red blotches on the head: a V- or Y-shaped blotch at the center of the frons and two symmetrical blotches on the temples.

Description of holotype. Head-to-elytron length (frons anterior margin to elytra posterior extreme): 16.3 mm. Total length (including abdomen): 42.5 mm. Maximum width (distance between elytra outer extremes): 9.2 mm. Body robust. Voluminous and elongated abdomen. Reduced and convex elytra, hindwings absent. Coloration black all over body and appendages except for head, which features two symmetrical red to orange blotches over temples, and a single, isolated smaller Y-shaped blotch at center of frons (Fig. 11). Tibial spines and pretarsal claws brownish. Black setae dispersed over body, very scattered on dorsal areas of head, thorax and abdomen. Tegument finely microreticulated, semimatt. — ***Head***: voluminous, broadly rounded and slightly wider than pronotum (head maximum width: 4.9 mm). Temples very wide and regularly rounded. Surface sparsely covered by very small to medium-sized punctures, homogeneously distributed, rounded, finely impressed, isolated from each other. A longitudinal midline finely impressed from apical half of frons to vertex. Frontal side of cephalic capsule slightly curved, with surface above antennal insertions slightly elevated and disc region almost flat, subconvex. Frons and temples almost glabrous, with a very short seta (almost inappreciable) on some punctures, especially on upper margin of antennal insertion. Occiput with moderately long and decumbent setae. Postocciput (sclerotized region between occiput and pronotum) laminar, semilunar, conspicuous, dense, and deeply punctate, also with moderately long and decumbent setae. Eyes small, kidney-shaped and weakly swollen, with dorsal and ventral lobes of similar size; barely notched at level of antennal insertions; minimum interorbital distance: 2.8 mm. Frontoclypeal suture deeply marked, arcuate. Clypeus flat, subtriangular, transverse (2.7 mm wide by 1.3 mm long); punctures small and separated; long setae homogeneously distributed following puncture pattern, directed forward, longer in sides. Labrum-clypeus suture almost straight. Labrum transverse (2.4 mm wide by 1.2 mm long), slightly emarginated in middle; punctures similar to those of clypeus; setae longer in lobes, following puncture pattern, oriented forward and curved towards center. Mandibles robust, longitudinally concave on outer side and notched in its distal region, glabrous in apex, and basally pilose. Maxillary palpi with palpomere I longer than others, subtroncoconical; II short, subcylindrical; III subtrapezoidal and dorso-ventrally flattened; distal palpomere widest with a narrow excavation along distal margin; pilosity moderately long in palpomeres I and II, shorter on distal palpomere. Labial palpi with palpomere I subcylindrical; II troncoconical; III subtrapezoidal, with pilosity as on maxillary palpi. Antennae 11-segmented, subcompressed, not reaching pronotum base when extended backward. Antennomeres dilated apically, with short black vestiture, mostly decumbent and with a few sparse setae erect, longer and semi-erect on scape and pedicel; scape (length: 0.7 mm) slightly dilated apically, subcylindrical; pedicel (length: 0.2 mm) very short, subglobose; antennomere III (length: 0.9 mm) subcylindrical, slightly dilated apically, rectangular; IV (length: 0.9 mm) similar to III, subrectangular; V (length: 0.8 mm) trapezoidal, wider than VI, with a wide and smooth apical tooth on inner edge; VI (length: 0.7 mm) trapezoidal, with smooth apical tooth on inner edge, not as prominent as those in V and VII; VII (length: 0.7 mm) trapezoidal, wider than VI, with an acute and prominent apical tooth on inner edge; VIII (length: 0.6 mm) trapezoidal, weakly dentate on apex of inner edge; IX (length: 0.7 mm) trapezoidal, dentate on inner edge; X (length: 0.6 mm) trapezoidal, apical tooth slightly acute; XI (length: 0.8 mm) subconical, slender, slightly notched on apex, ending in an elongated tooth. — ***Thorax***: Pronotum subquadrate with subparallel sides, narrower posteriorly (anterior side of pronotum: 4.2 mm; posterior margin of pronotum: 3.6 mm; pronotum length on sagittal plane: 3.4 mm); anterior margin concavely curved, posterior margin slightly convexly arcuate; fore angles acute, hind angles rounded; surface weakly convex at its central area, with a fine impressed longitudinal midline, and with shallow and diffuse lateral depressions. Pronotal base entire and finely bordered. Pronotal surface irregularly punctate; punctures of various sizes, from small to large sizes, circular and relatively deep; disc area only with small punctures; large punctures close but mostly isolated from each other, distributed on anterior and lateral sides and bordering anterior midline portion. Punctures do not form a corrugated or reticulated pattern. Dorsal surface of pronotum almost glabrous, with an isolated short seta in each puncture; anterior margin, adjacent to post-occiput, with numerous setae, moderately long. Mesonotum covered mostly by pronotum, showing only its posterior margin, straight and strongly punctate, with longitudinal wrinkles. Metanotum completely covered by elytra. Prosternum narrow, slightly extended posteriorly, pointed at tip. Mesosternum with a triangular prolongation, extended posteriorly, ending

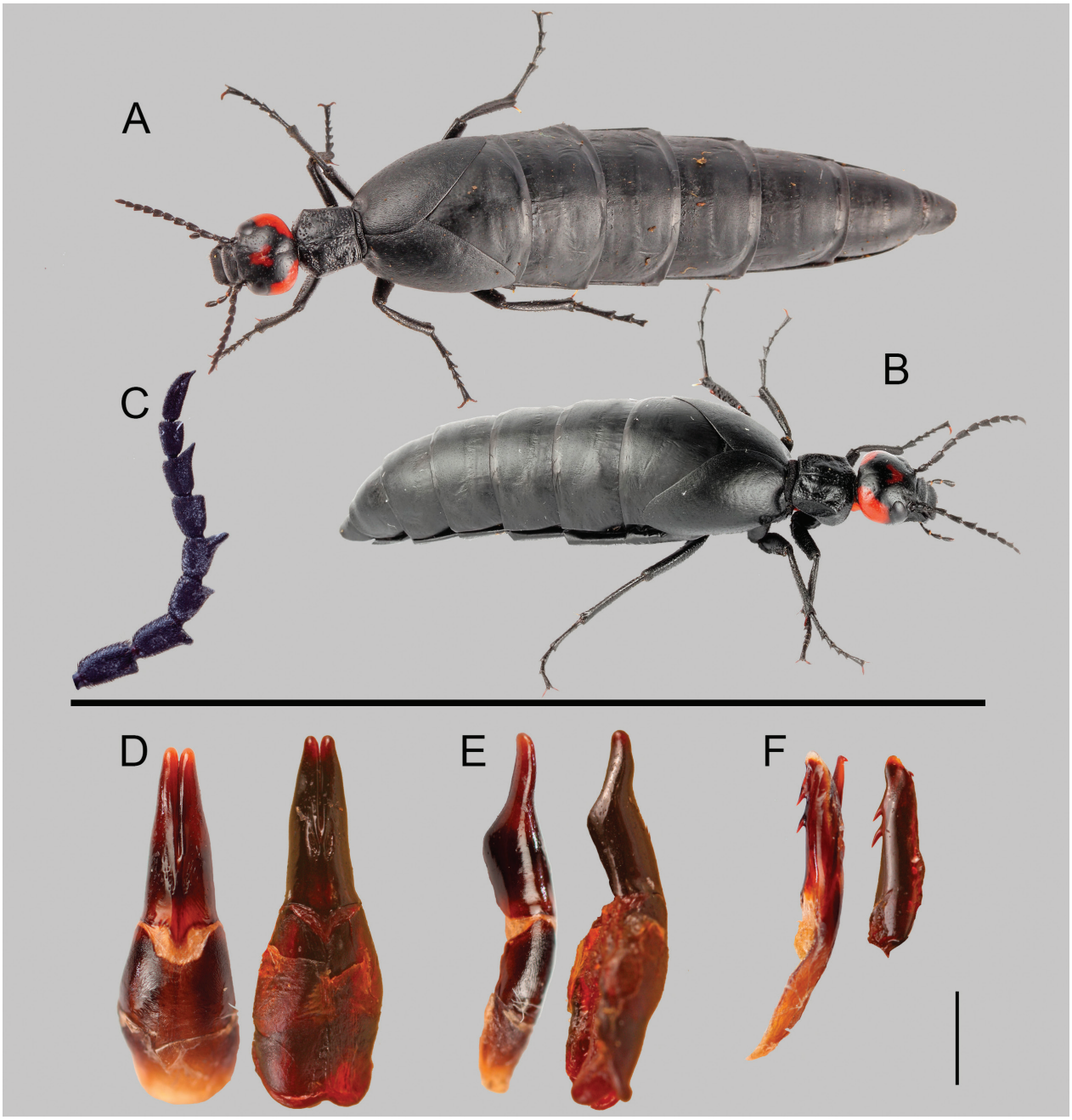

Figure 11. *Berberomeloe insignis trisanguinatus* **ssp. nov.** Female from Tabernas, Almería (**A**). Male Holotype (MNCN_Ent 429880) from Escúllar, Sierra de los Filabres, Almería (**B**). Male antennomeres IV–XI from a specimen from Tabernas (**C**). Male genitalia (**D–F**): ventral view of the gonoforceps (**D**) (right: holotype; left: specimen from Tabernas, Almería); lateral view of the gonoforceps (**E**) (right: holotype; left: specimen from Tabernas, Almería); lateral view of the aedeagus (**F**) (right: holotype; left: specimen from Tabernas, Almería); scale bar: 1 mm.

in a rounded tip that extends to level of apical half of mesocoxae; lateral extensions narrow; surface covered by disperse short setae. Metasternum subtrapezoidal, wide, with a prolongation extended posteriorly, ending in an emarginated tip. — ***Elytra***: reduced and convex, imbricated basally, longer than pronotum (length: 9 mm), divergent posteriorly and reaching posterior portion of abdominal tergite II; tegument glabrous, slightly corrugated longitudinally with no marked punctures. — ***Legs***: moderately robust, covered by decumbent and relatively long setae. Mesotrochanters and -coxae overlap partially with metacoxae. Metafemur shorter than metatibia (metafemur length: 5 mm; metatibia length: 5.3 mm). Pro- and mesotibiae with two similar spurs, slender and straight; metatibial spurs dissimilar and divergent; inner spur spatulated, outer spur similar to those of pro- and mesotibiae. Tarsi long, with tarsomeres subcylindrical, slightly expanded distally and emarginated. Protarsi shorter than meso- and metatarsi. Metatarsomere I large, followed in size by II and IV (length of metatarsomeres: from basal to apical tarsomere: 2.6, 1.3, 1.0, 1.4 mm). Tarsal ventral pads consisting of a dense, short and thick tuft of semi-erected setae. Metatarsomeres with relatively thick setae, distributed longitudinally through dorsal

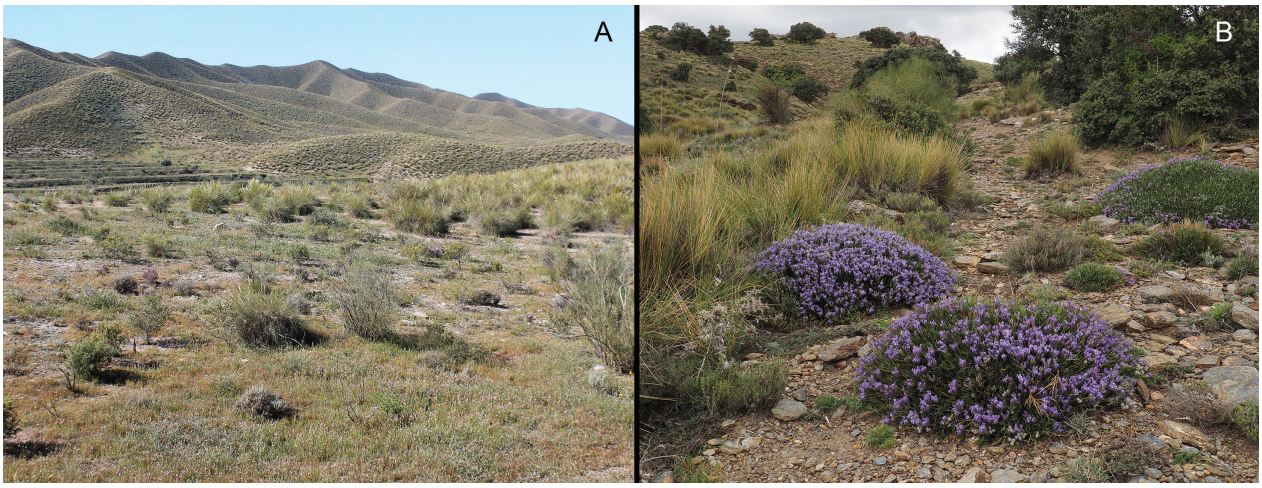

Figure 12. Habitats of *Berberomeloe insignis trisanguinatus* **ssp. nov.** Environment from Tabernas to Turrillas, Almería (**A**). Landscape of the highest known locality for *B. insignis trisanguinatus*, in the surroundings of El Haza de Riego, North of Escúllar, Sierra de los Filabres, Almería (**B**).

side of each tarsomere. Claws smooth, curved, with lower lobe narrower and smaller. — ***Abdomen***: voluminous, entirely black. Tergite I mostly covered by elytra. Dorsal surface of abdomen smooth, almost glabrous, with scarce, small, and shallow punctures with a very short seta on each puncture. Posterior margin of last visible tergite VIII with dense short setae. Ventrites with sparse and slightly marked punctures mostly on posterior half, with very short and decumbent black setae, scattered but homogeneously distributed. Last ventrite VIII notched at its posterior margin. — ***Male genitalia***: (Fig. 11D–F) with gonoforceps brownish, 3 mm long, 1 mm wide; moderately elongated, relatively slender both in dorsal and lateral views. Gonocoxal plate longer than wide, a little less long than gonostyli, wider on dorsal view; maximum width in middle part. Gonostyli longer than wide, basally cylindrical; basal 1/3 fused; scarce setae, applied against tegument present on middle dorsal region of gonostyli. Gonostyli lobes separated by a longitudinal notch that extends to middle of dorsal surface of gonostyli; apices rounded, digitiform. Aedeagus long, robust, flattened, truncated at apex, with two acute dorsal hooks, subequal, close to each other and separated from apex. Endophallic hook visible.

Variability. Body length (frons to posterior margin of elytra) ranges from 9 to 24 mm. Red-orange mark on frons varies in shape, ranging from a V- to Y-like.

Females last abdominal ventrite VIII rounded, not emarginated at its posterior margin, with antennomeres V, VII, and IX less widened apically, and last antennomere XI less slender in its inner apical portion than in males.

Diagnosis and comparisons. *Berberomeloe insignis trisanguinatus* **ssp. nov.** can be readily differentiated from other taxa of the *B. insignis* species group by the presence of (1) two symmetric red- to orange-colored blotches over the temples that do not extend anteromedially as a lobate projection above the ocular margin, and (2) a single, isolated, V- or Y-shaped mark on the frons (Fig. 11A, B).

Berberomeloe insignis trisanguinatus can also be differentiated from *B. nazari* **sp. nov.** by the different shape of male antennomeres VII, IX and XI, which are more elongated in *B. insignis trisanguinatus*. From *B. insignis insignis* it can be distinguished by the shape of female and male antenomeres VII–XI, which are shorter in *B. insignis trisanguinatus* compared to *B. insignis insignis*. Beyond the presence of a frontal red blotch on the head, the only morphological difference between *B. insignis trisanguinatus* and the specimens of the C2 lineage is found in the male antennomere VII (Table S5).

Distribution and notes on natural history. Endemic to the province of Almería. Populations of *B. insignis trisanguinatus* are distributed across eastern and central Almería, with coastal and inland populations, particularly in the Tabernas Desert and Pasillo de Fiñana region, situated between Sierra Nevada and Sierra de los Filabres. It is an element of low to mid altitudes, with an altitudinal range from sea level to 1800 m a.s.l. It mainly occupies the thermo-Mediterranean bioclimatic level and, occasionally, extends into the meso-Mediterranean zone, and more rarely into the supra-Mediterranean zone, in the latter cases in areas of high temperature and low rainfall. The dominant ombroclimate in its distribution area is semi-arid (250–400 mm of average annual rainfall) (e.g., Alcaraz and Peinado 1987; Rivas-Martínez 1987, 2007; Valle 2003). *Berberomeloe insignis trisanguinatus* primarily inhabits steppic or submontane environments with sparse shrubby or xeric scrub vegetation and little to no tree cover. Typical habitats include steppes dominated by *Macrochloa tenacissima* (L.) Kunth or uncultivated areas with *Retama sphaerocarpa* (L.) Boiss., and *Anthyllis cytisoides* L., often near cultivated fields with almond trees (Fig. 12). It has been found in Sierra de los Filabres, at an altitude of 1800 m a.s.l. around Haza de Riego, situated between Escúllar and Puerto de Escúllar. The vegetation in this area is dominated by dispersed trees of *Quercus rotundifolia* Lam. and *Cytisus* Desf. (Fig. 12). Adults have been reported feeding on flowers of *Convolvulus* (García-

París et al. 1999) and leaves of Asteraceae (Sánchez-Vialas pers. obs.).

Berberomeloe insignis trisanguinatus has been found in sympatry with *B. indalo* in the following localities of Almería: El Puntal (García-París et al. 1999), Peñas Negras (García-París et al. 1999), Rambla Seca de Tabernas (García-París et al. 1999), and between Tabernas and Turrillas (Sánchez-Vialas pers. obs.).

Berberomeloe nazari Sánchez-Vialas, Calatayud-Mascarell, Ruiz, Recuero, and García-París, sp. nov. (C1 lineage)

https://zoobank.org/BE6FF692-A9FF-4F8F-8F26-E259A59C4420

Type material. Holotype: Male, labeled: Spain, Málaga, Río de la Miel, 36°47′40.9″N 03°46′24.5″W, 16-IV-2024, Sánchez Vialas, A. leg. [white label, printed]; MNCN_Ent 429955 [white label, printed]; Holotypus, *Berberomeloe nazari* Sánchez-Vialas, Calatayud-Mascarell, Ruiz, Recuero, & García-París des. 2025 [white label, printed]. Preserved in absolute ethanol at the Entomological collection of the Museo Nacional de Ciencias Naturales, Madrid. — **Paratypes** (34 exx, all held at the Entomological collection of the Museo Nacional de Ciencias Naturales, Madrid): 1 male and 5 females. labeled: Málaga, Río de la Miel, 36°47′40.9″N 03°46′24.5″W, 16-IV-2024, Sánchez Vialas, A. leg. [white label, printed]; MNCN_Ent 429956–429961 [white label, printed] (preserved in ethanol). – 1 male and 1 female, labeled: Málaga, Río de la Miel, 36°47′32.23″N 03°46′09.81″W, 22-V-2021, J. L. Ruiz leg. [white label, printed]; MNCN_Ent 429965 [white label, printed] (preserved together in ethanol). – 3 females, labeled: Málaga, Río de la Miel, 36°47′32.23″N 03°46′09.81″W, 22-V-2021, J. L. Ruiz leg. [white label, printed]; MNCN_Ent 429966, 429967, 429964 [white label, printed]; ASV2201, ASV2202, ASV21008 [white label, handwritten] (preserved in ethanol). – 1 male, labeled: Málaga, Torre de Maro, 07-IV-2021, J. L. Ruiz leg. [white label, printed]; MNCN_Ent 429963 [white label, printed]; ASV21006 [white label, handwritten] (preserved in ethanol). – 2 males, labeled: Granada, Jete, 36°47′34.93″N 03°39′05.73″W, 09-III-2021, Sánchez Vialas, A. leg. [white label, printed]; ASV21003-ASV21004 [white label, handwritten]; MNCN_Ent 429973–429974 [white label, printed] (males, preserved in ethanol). – 1 male, labeled: Jete, Granada, 36°48′11.60″N 03°39′34.50″W, 16-III-2020, François, A. leg. [white label, printed]; ASV21001 [white label, handwritten]; MNCN_Ent 429976 [white label, printed] (preserved in ethanol). – 1 female, labeled: Jete, Granada, 36°48′11.60″N 03°39′34.50″W, 10-IV-2020, François, A. leg. [white label, printed]; MNCN_Ent 429975 [white label, printed]; ASV21002 [white label, handwritten] (preserved in ethanol). – 1 female, labeled: Jete, Granada, 36°48′11.60″N 03°39′34.50″W, 09-IV-2021, François, A. leg. [white label, printed]; MNCN_Ent 429962 [white label, printed] (preserved in ethanol). – 1 female, labeled: Granada, 3 km southern Polopos, 36°45′48.48″N 03°18′07.61″W, 11-IV-2010, García-París, M. & Bologna, M.A. leg. [white label, printed]; MNCN_Ent 429971 [white label, printed] (preserved in ethanol). – 1 male, labeled: Granada, 4 km southern Polopos, 36°45′26.01″N 03°17′56.09″W, 11-IV-2010, García-París, M. & Bologna, M.A. leg. [white label, printed]; MNCN_Ent 429972 [white label, printed] (preserved in ethanol). – 6 males and 9 females, labeled: Granada, La Garnatilla to Lújar, 36°43′42.05″N 03°26′27″W, 06-V-2018, Calatayud, A. & Tena, J. leg. [white label, printed]; MNCN_Ent 429968 (shared among 13 specimens), MNCN_Ent 429969, MNCN_Ent 429970 [white label, printed] (preserved in ethanol). All paratypes labeled: 'Paratypus, *Berberomeloe nazari* Sánchez-Vialas, Calatayud-Mascarell, Ruiz, Recuero, & García-París des. 2025' [white labels, printed].

Etymology. The specific epithet "*nazari*" refers to the Kingdom of Granada under the Nasrid dynasty (Banū Naṣr), the last Muslim dynasty to rule Al-Andalus (13th–15th century). The name highlights the historical and cultural significance of the region, as the species is distributed across Granada and the eastern limits of Málaga, areas that once formed part of the Nasrid domain.

Description of the holotype. Head-to-elytron length (frons anterior margin to elytra posterior extreme): 18.4 mm. Total length (including abdomen): 39 mm. Maximum width (distance between elytra outer extremes): 11.6 mm. Body robust. Voluminous and elongated abdomen. Reduced and convex elytra, hindwings absent. Coloration black all over body and appendages except for head, which features 2 symmetrical red to orange blotches over temples that extends into frons (but not reaching frons midline) after bordering the upper ocular margin area (Fig. 13). Tibial spines and pretarsal claws brownish. Black setae dispersed over body, very scattered on dorsal areas of head, thorax and abdomen. Tegument finely microreticulated, semimatt. — ***Head***: Voluminous, broadly rounded and slightly wider than pronotum (head maximum width: 5.7 mm). Temples very wide and regularly rounded. Surface sparsely covered by very small to medium-sized punctures, homogeneously distributed, rounded, finely impressed, isolated from each other. A longitudinal midline is finely impressed from apical half of frons to vertex. Frontal side of cephalic capsule slightly curved, with surface above antennal insertions slightly elevated and disc region almost flat, subconvex. Frons and temples almost glabrous, with a very short seta (almost inappreciable) on some punctures, especially on anterior margin of antennal insertion. Occiput with moderately long and decumbent setae. Postocciput laminar, semilunar, conspicuous, dense and deeply punctate, also with moderately long and decumbent setae. Eyes small, kidney-shaped and weakly swollen, with dorsal and ventral lobes of similar size; barely notched at level of antennal insertions; minimum interorbital distance: 3.2 mm. Frontoclypeal suture between frons and clypeus deeply marked, arcuate. Clypeus flat, subtriangular, transverse (2.8 mm wide by 1.2 mm long); punctures small and separated; long setae homogeneously distributed following puncture pattern, directed forward, longer in sides. Labrum-clypeus suture almost straight. Labrum transverse (2.7 mm wide by 1.6 mm long), slightly emarginated in middle; punctures similar to those of clypeus; setae longer in lobes, following puncture pattern, oriented forward and curved towards center. Mandibles robust, longitudinally concave on outer side and notched in its distal region, glabrous in apex, and basally pilose. Maxillary palpi with palpomere I longer than others, subtroncoconical; II short, subcylindrical; III subtrapezoidal and dorso-ventrally flattened; distal

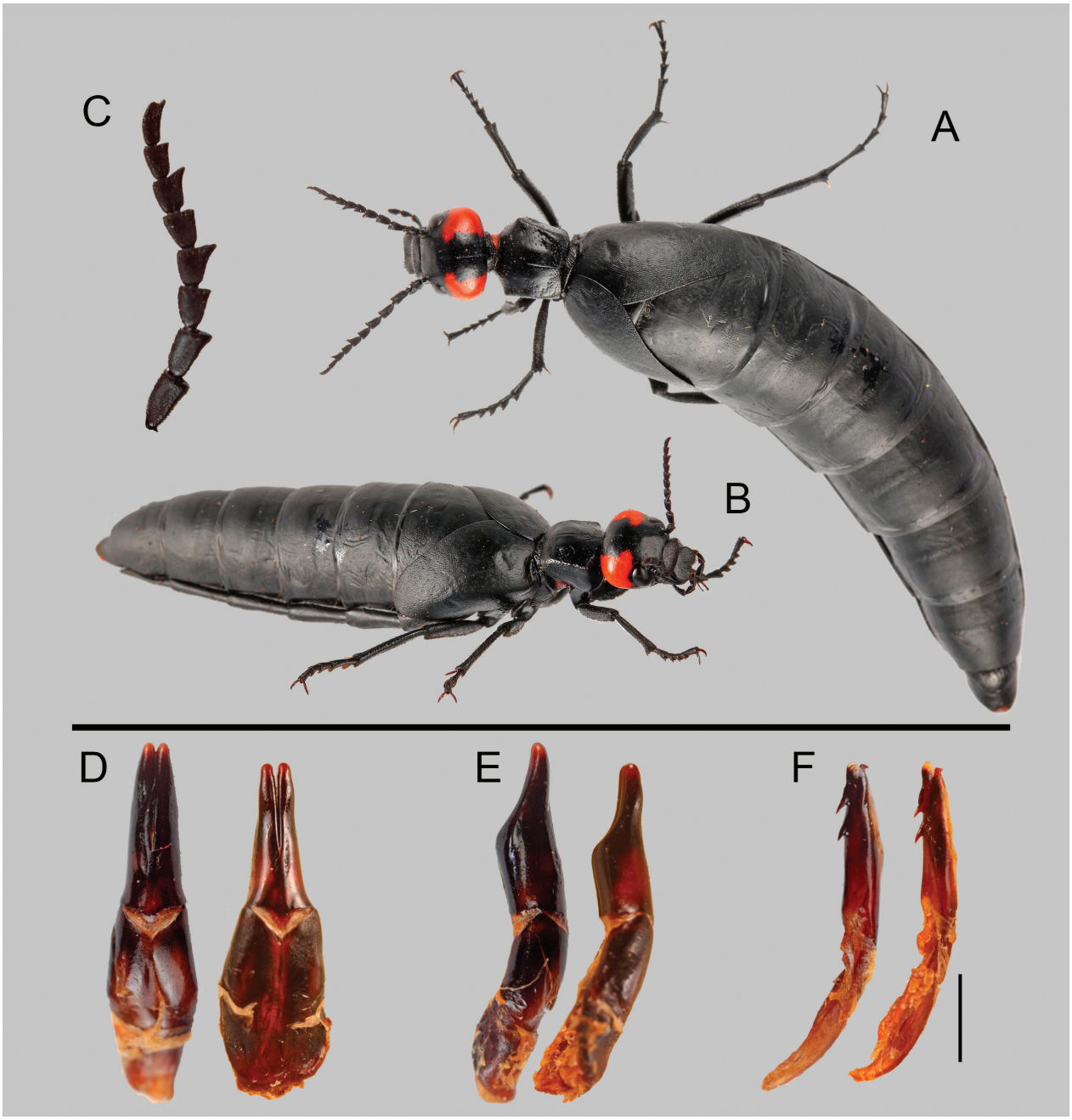

Figure 13. *Berberomeloe nazari* **sp. nov.** Dorsal and dorsolateral views of the same specimen from Lújar, Granada (**A**, **B**). Male antennomeres IV–XI from a specimen from La Garnatilla to Lújar (**C**). Male genitalia (**D**–**F**): ventral view of the gonoforceps (**D**) (right: holotype; left: specimen from La Garnatilla, Granada); lateral view of the gonoforceps (**E**) (right: holotype; left: specimen from La Garnatilla, Granada); lateral view of the aedeagus (**F**) (right: holotype; left: specimen from La Garnatilla, Granada); scale bar: 1 mm.

palpomere widest with a narrow excavation along distal margin; pilosity moderately long in palpomeres I and II, shorter on distal palpomere. Labial palpi with palpomere I subcylindrical; II troncoconical; III subtrapezoidal, with pilosity as on maxillary palpi. Antennae 11-segmented, subcompressed, not reaching pronotum base when extended backward. Antennomeres dilated apically, with short black vestiture, mostly decumbent and with a few sparse setae erect, longer and semi-erect on I–II segments; scape (length: 0.9 mm) slightly dilated apically, subcylindrical; pedicel (length: 0.3 mm) very short, subglobose; antennomere III (length: 1.1 mm) subcylindrical, slightly dilated apically, rectangular; IV (length: 1.1 mm) similar to III, subrectangular; V (length: 1 mm) trapezoidal, wider than VI, with a wide and smooth apical tooth on inner edge; VI (length: 0.8 mm) trapezoidal, with a wide and smooth apical tooth on inner edge; VII (length: 0.8 mm) trapezoidal, wider than VI, with an acute apical tooth on inner edge; VIII (length: 0.7 mm) trapezoidal, weakly dentate on apex of inner edge; IX (length: 0.7 mm) trapezoidal, dentate on inner edge; X (length: 0.6 mm) trapezoidal, apical tooth slightly acute; XI (length: 0.9 mm) subconical, notched on apex. — ***Thorax***: Pronotum subquadrate with subparallel sides, narrower posteriorly

(anterior side of pronotum: 5.2 mm; posterior margin of pronotum: 4.2 mm; pronotum length on sagittal plane: 4.2 mm); anterior margin concavely curved, posterior margin slightly convexly arcuate; fore angles acute, hind angles rounded; surface weakly convex at its central area, with a fine impressed longitudinal midline, and with shallow and diffuse lateral depressions. Pronotal base entire and finely bordered. Pronotal surface irregularly punctate; punctures of various sizes, from small to large sizes, circular and relatively deep; disc area only with small punctures; large punctures close but mostly isolated from each other, distributed on anterior and lateral sides and bordering anterior mid-line portion. Punctures do not form a corrugated or reticulated pattern. Dorsal surface of pronotum almost glabrous, with an isolated short seta in each puncture; anterior margin, adjacent to post-occiput, with numerous setae, moderately long. Mesonotum covered mostly by pronotum, showing only its posterior margin, straight and strongly punctate, with longitudinal wrinkles. Metanotum completely covered by elytra. Prosternum narrow, slightly extended posteriorly, pointed at tip. Mesosternum with a triangular prolongation, extended posteriorly, ending in a rounded tip that extends to level of anterior half of mesocoxae; lateral extensions narrow; surface covered by disperse short setae. Metasternum subtrapezoidal, wide, with a prolongation extended posteriorly, ending in an emarginated tip. — ***Elytra***: Reduced and convex, imbricated basally, longer than pronotum (length: 10.7 mm), divergent posteriorly and reaching posterior half of abdominal tergite II; tegument glabrous, slightly corrugated longitudinally with no marked punctures. — ***Legs***: Moderately robust, covered by decumbent and relatively long setae. Meso-trochanters and coxae overlap partially metacoxae. Metafemur shorter than metatibia (metafemur length: 6.3 mm; metatibia length: 6.1 mm). Pro- and mesotibiae with 2 similar spurs, slender and straight; metatibial spurs dissimilar and divergent; inner spur spatulated, outer spur similar to those of pro- and mesotibiae. Tarsi long, with tarsomeres subcylindrical, slightly expanded distally and emarginated. Protarsi shorter than meso- and metatarsi. Metatarsomere I large, followed in size by II and IV (length of metatarsomeres: from inner to apical segment: 3.1, 1.5, 1.3, 1.7 mm). Tarsal ventral pads consisting on a dense, short and thick tuft of semi-erected setae. Metatarsomeres with relatively thick setae, distributed longitudinally through dorsal side of each tarsomere. Claws smooth, curved, with lower lobe narrower and smaller. — ***Abdomen***: Voluminous, entirely black. Tergite I partly covered by elytra. Dorsal surface of abdomen smooth, almost glabrous, with scarce, small, and shallow punctures with a very short seta on each puncture. Posterior margin of last visible tergite with dense short setae. Ventrites with sparse and slightly marked punctures mostly on posterior half, with very short and decumbent black setae, scattered but homogeneously distributed. Last ventrite notched at its posterior margin. — ***Male genitalia*** (Fig. 13D–F): Gonoforceps brownish, 4 mm long, 1.4 width; moderately elongated, relatively slender both on dorsal and lateral views. Gonocoxal plate longer than wide, a little less long than gonostyli, wider on dorsal view; maximum width in middle part. Gonostyli longer than wide, basally cylindrical; basal 1/3 fused; scarce setae, applied against tegument present on middle dorsal region of gonostyli. Gonostyli lobes separated by a longitudinal notch that extends to middle of dorsal surface of gonostyli; apexes rounded, digitiform. Aedeagus long, robust, flattened, truncated at apex, with two acute dorsal hooks, subequal, close to each other and separated from apex. Endophallic hook visible.

Variability. Body length (frons to posterior margin of elytra) from 11 to 22 mm. Female last abdominal ventrite VIII rounded, not emarginated at its posterior margin, with antennomeres V, VII, and IX less widened apically, and last antennomere not dentate in its inner apical portion.

Diagnosis and comparisons. *Berberomeloe nazari* **sp. nov.** can be readily differentiated from other taxa of the *B. insignis* species group by the presence of (1) two symmetric red- to orange-colored blotches on the temples, each with its inner margin extending anteromedially as a lobate projection above the ocular margin, partially approaching the frons but not reaching the midline, which remains entirely black, (2) the absence of a V- or Y-shaped mark on the frons, and (3) male antennomere XI wide and notched in its posterior margin (Fig. 13).

See accounts of *B. insignis insignis*, *B. insignis trisanguinatus* for morphological comparisons with this taxon. No additional morphological differences were observed between *B. nazari* and the specimens belonging to the C2 lineage.

Distribution and notes on natural history. *Berberomeloe nazari* ranges from Torre de Maro (Nerja) in eastern Málaga to the western border of Almería. This species generally occupies highly rugged terrain, characteristic of the Sierra de la Contraviesa, Sierra de Lújar, the southern boundary of the Sierra de la Almijara, and the southern slopes of Sierra Nevada (Fig. 14). It has been recorded across an altitudinal range between the sea level and 1090 m a.s.l. in Laujar de Andarax and Yegen (southern slopes of Sierra Nevada). It primarily inhabits the thermo-Mediterranean bioclimatic zone and, to a lesser extent, the meso-Mediterranean, in areas with a predominantly dry ombrotype (average annual rainfall of 400–600 mm) and occasionally subhumid conditions (600–700 mm) (see Valle 2003; Rivas-Martínez 2007). In this regard, this lineage is found in less arid regions compared to the others discussed. The habitats it inhabits vary greatly, ranging from areas dominated by scattered patches of trees such as *Quercus suber* L., *Q. faginea* Lam., *Q. rotundifolia*, *Pinus halepensis* Mill., and *Ceratonia siliqua* L., along with shrubs of the genus *Cistus* L. in the Sierra de Lújar, to drier landscapes dominated by olive and almond orchards across much of the Alpujarra range and eastern Málaga (Fig. 14). Our findings extend the distribution range of this species group further westwards, providing the first documented records in the province of Málaga.

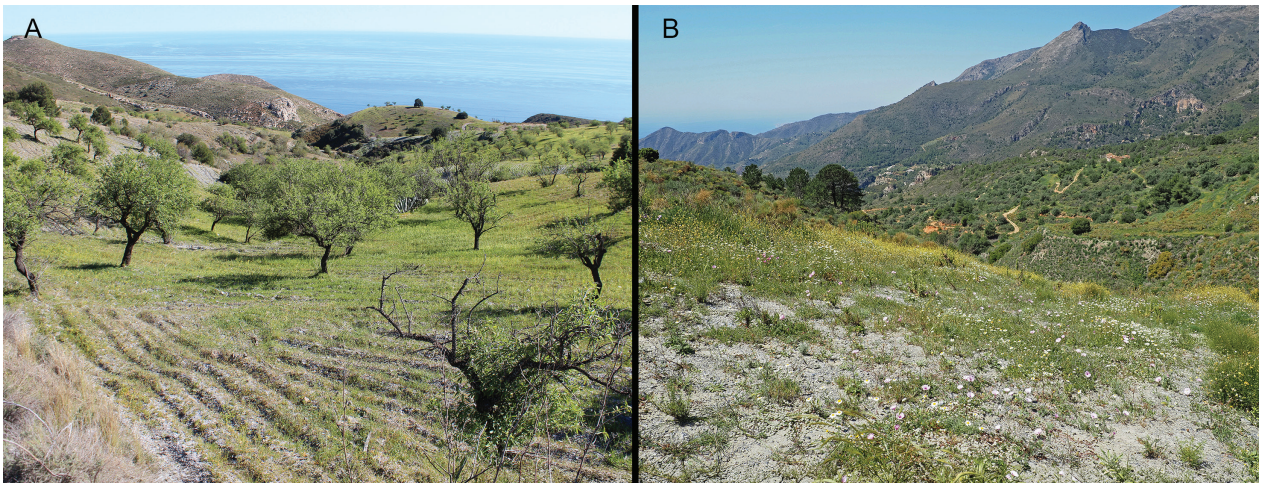

Figure 14. Habitats of *Berberomeloe nazari* **sp. nov.** Landscape between La Garnatilla and Gualchos, Granada (**A**). Surroundings of Río de la Miel, El Rescate, northeast of Maro, Málaga (**B**).

Populations of the "C2" lineage

Material examined. (45 exx). 5 males, 1 female, labeled: S. Felix, Almería, Spain, 36°51′45.0″N 2°39′43.6″W, 17-IV-2024, Sánchez Vialas, A. leg. [white label, printed]; MNCN_Ent 429910–429915 [white label, printed]. – 12 males and 18 females, labeled: Spain, Almería, 5Km SW Las Marinas, 7 m, 36°42′65.00″N 02°40′17.3″W, 30-III-2008, E. Recuero & C. Settanni leg. [white label, printed]; BI013, 287, 292–294, 296, 298, 302, 304, 310, 312, 314, 001–006, 289–291, 295, 297, 299–301, 303, 305, 309, 313 [white label, handwritten]; MNCN_Ent 429916–429941, MNCN_Ent 429954, MNCN_Ent 429942–429944 [white label, printed] (preserved in ethanol). – 1 female, labeled: Faro del Sabinar-Las Marinas, 7 Km, Ctra a San Agustín, borde de las salinas, 1 m, 36°41′80.03″N 02°42′19.5″W, 29-III-2008, E. Recuero & C. Settanni leg. [white label, printed]; ASV18011 [white label, handwritten]; MNCN_Ent 429949 [white label, printed] (preserved in ethanol). – 2 females and 3 males, labeled: Faro del Sabinar-Las Marinas, 7 Km, Ctra a San Agustín, borde de las salinas, 1 m, 36°41′80.03″N 02°42′19.5″W, 29 March 2008, E. Recuero & C. Settanni leg. [white label, printed]; BI007–008, BI14–15 [white label, handwritten]; MNCN_Ent 429950–429953 [white label, printed] (preserved in ethanol). – 3 females and 1 male, labeled: 2Km W Las Marinas, Ctra a San Agustín, borde de las salinas, 13 m, 36°43′10.08″N 02°39′41.7″W, 29-III-2008, E. Recuero & C. Settanni leg. [white label, printed]; BI009–BI012 [white label, handwritten]; MNCN_Ent 429945–429948 [white label, printed] (preserved in ethanol).

Diagnosis and comparisons. These populations can be differentiated from other taxa by the presence of (1) two symmetric red- to orange-colored blotches over the temples that typically do not extend anteromedially as a lobate projection above the ocular margin (but see variability), (2) the absence of a clearly defined V- or Y-shaped mark on the frons, and (3) a relatively wide separation of both temples blotches at occiput level (Figs 15, 16).

See the account of *B. insignis insignis* for morphological comparisons with this lineage. Beyond the cephalic phenotype, no additional morphological differences were observed between *B. nazari* **sp. nov.** and *B. insignis trisanguinatus* **ssp. nov.**

Variability. Body length (frons to posterior border of elytra) from 10 to 25 mm. Shape of the last male antennomere highly variable, ranging from notched at the apex to unnotched. Although typically exhibits a consistent pattern in head phenotype, as shown in Fig. 16D, some revised specimens (N = 4) from the southern slopes of Sierra de Gádor (Felix), present a small, poorly conspicuous red circular blotches on both sides of the frontal midline. These blotches can appear isolated (Fig. 16A, B) or in contact to the red temporal blotches (Fig. 16C). Additionally, one of them exhibit a single blurred red spot at center of the frons (Fig. 16B). In this regard, these patterns appear to be a remnant of past hybridization between clades C1 and B2, reflecting an inherited trait from historical (or current) gene flow in the region between Sierra de Gádor and Campo de Dalías. However, further molecular analyses are needed to confirm this hypothesis.

Females have the last abdominal ventrite rounded, not emarginated at its posterior margin, with antennomeres V, VII, and IX less widened apically, and the last antennomere not dentate in its inner apical portion.

Distribution and notes on natural history. Lineage C2 is endemic to the province of Almería. It occurs between Campo de Dalías and the southern slopes of Sierra de Gádor. In Campo de Dalías, lineage C2 is found within the Natural Park of Punta Entinas-Sabinar, where it inhabits the sandy soils dominated by *Juniperus phoenicea* L. and *Pistacia lentiscus* L. (Fig. 17A). In April 2024, a single recently died specimen was found in a vacant lot (36°42′54.6″N 2°47′40.6″W), surrounded by greenhouses and roads (Fig. 17B, C). This location is under threat from ongoing agricultural expansion, and it is likely to disappear in the near future. On the southern slopes of

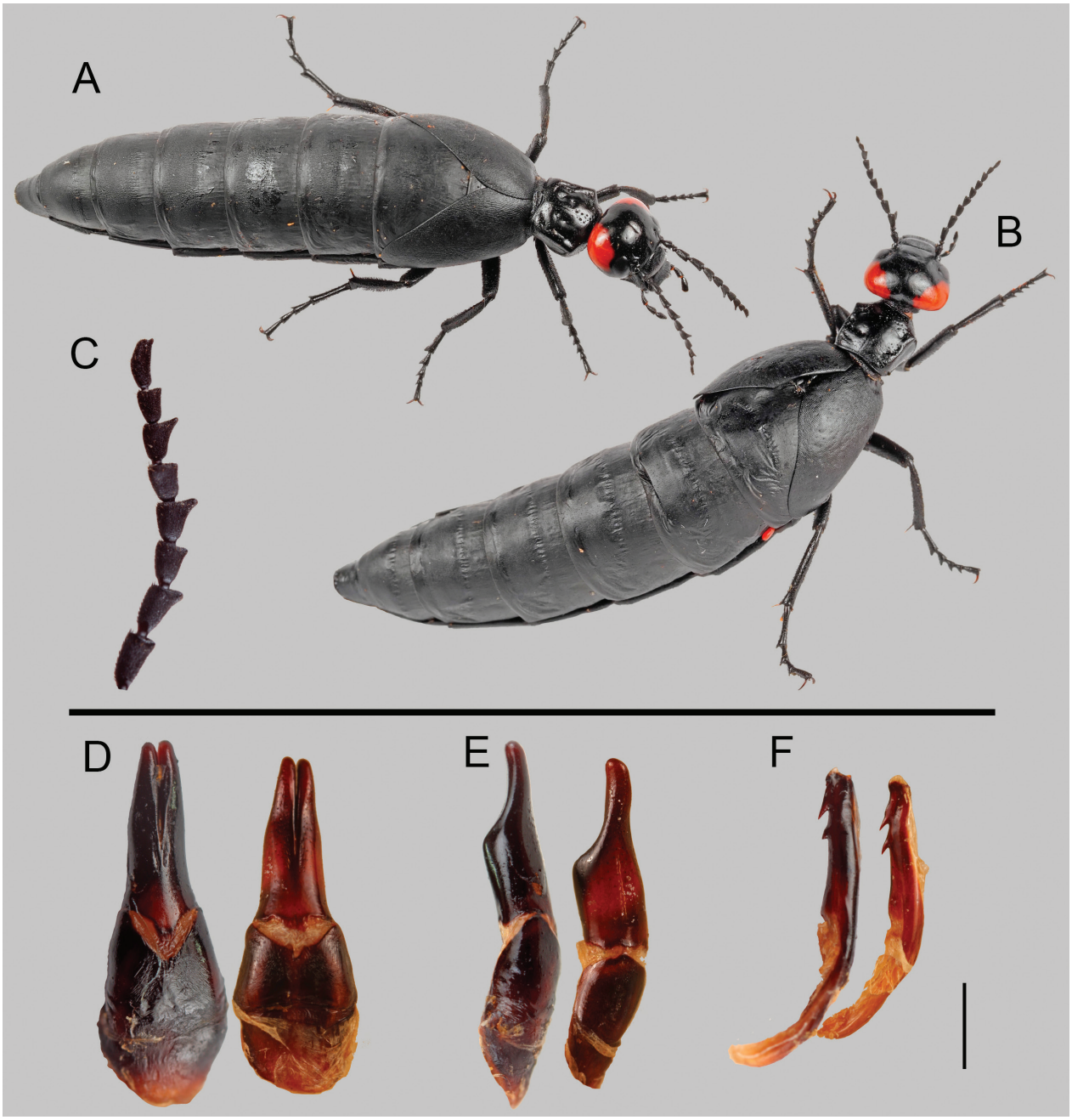

Figure 15. Specimens of *Berberomeloe* lineage C2. Male (MNCN_Ent 429910) and female (MNCN_Ent 429911) from South of Felix, Almería (**A**, **B**, respectively). Male antennomeres IV–XI from a specimen from southwest of Las Marinas, Almería (**C**) (other individuals from the same population lack the apical notch on antennomere XI). Male genitalia (**D**–**F**): ventral (**D**) and lateral (**E**) views of the gonoforceps (right: specimen from Felix; left: specimen from El Ejido, 5 km southwestern of Las Marinas, Almería); lateral view of the aedeagus (**F**) (right: specimen from Felix; left: specimen from El Ejido, 5 km southwestern of Las Marinas, Almería); scale bar: 1 mm.

Sierra de Gádor, it occurs in almond orchards and uncultivated areas dominated by *Retama sphaerocarpa* (Fig. 17D).

Three specimens housed in the entomological collection of the MNCN (MNCN_Ent 65241, MNCN_Ent 232555–MNCN_Ent 232557), labeled as originating from "Alquian" exhibit phenotypes consistent with this lineage. Notably, the revised specimens housed at the MUNA and collected near El Alquián, in the Cabo de Gata region, belong to *B. insignis trisanguinatus*, suggesting that the "Alquian" labels of the MNCN specimens may either refer to a locality closer to Campo de Dalías or result from mislabeling. Several populations once recorded in Campo de Dalías are now extinct due to habitat destruction caused by the rapid and extensive expansion of greenhouses across the region.

Figure 16. Phenotypic variability observed in *Berberomeloe* lineage C2 specimens from the same population at southern Felix (Sierra de Gádor, Almería). Specimen displaying two isolated orangish dots on either sides of the midline of the frons (**A**). Specimen with a similar pattern to A, but featuring an additional central, faint reddish blotch (**B**). Specimen where the small reddish blotches on either sides of the midline of the frons are connected to the main blotches of the temples (**C**). Specimen exhibiting the typical pattern observed in other populations, with no additional marks on the frontal surface (**D**).

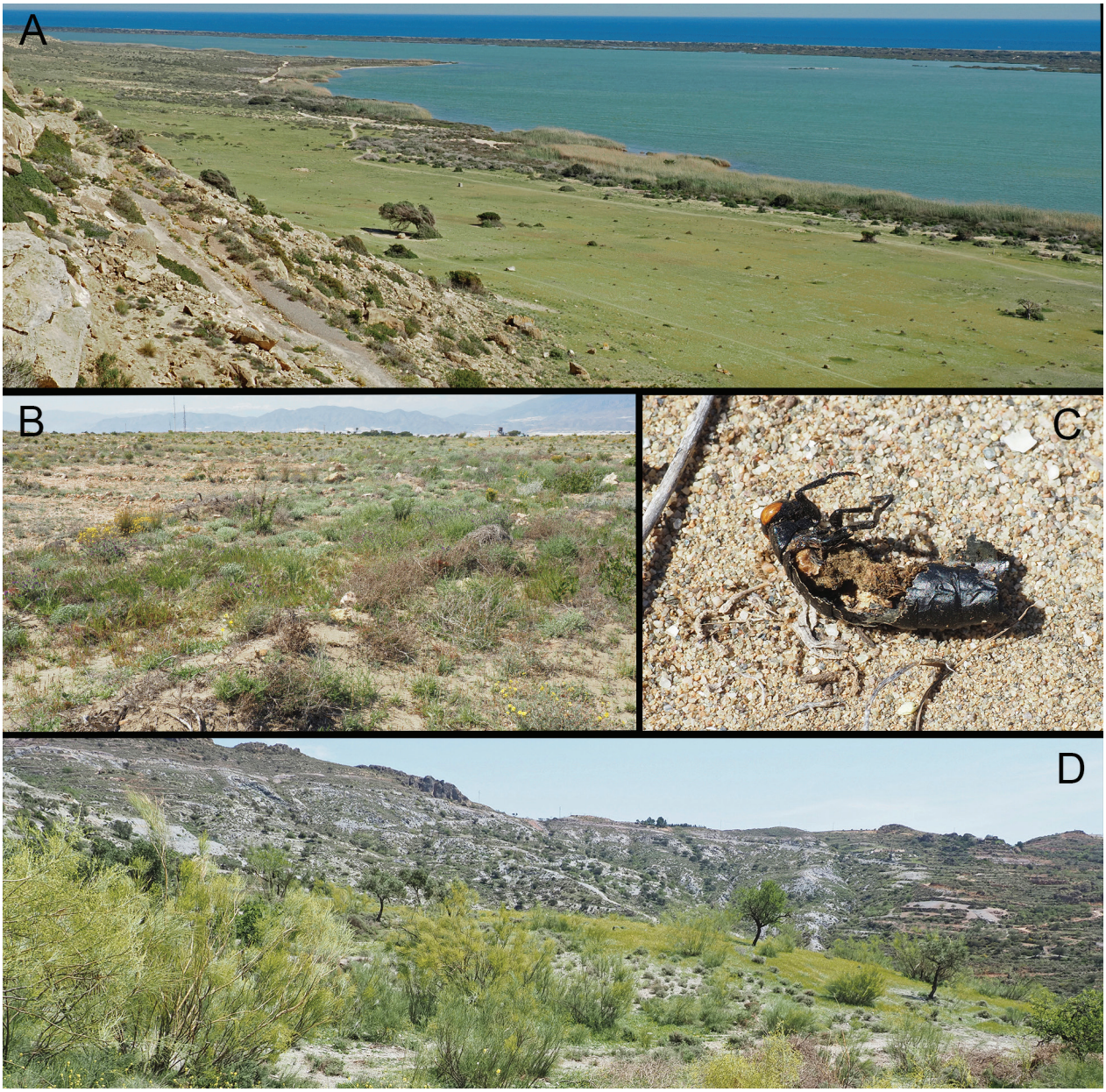

Figure 17. Habitat of *Berberomeloe* lineage C2 populations (**A**, **B**, **D**). Paraje Natural Punta Entinas-Sabinar, Almería (**A**). Vacant lot surrounded by greenhouses and roads, in El Ejido region, North of Almerimar, Almería (**B**). Carcass of a specimen found in B (**C**). South of Felix, Sierra de Gádor, Almería (**D**).

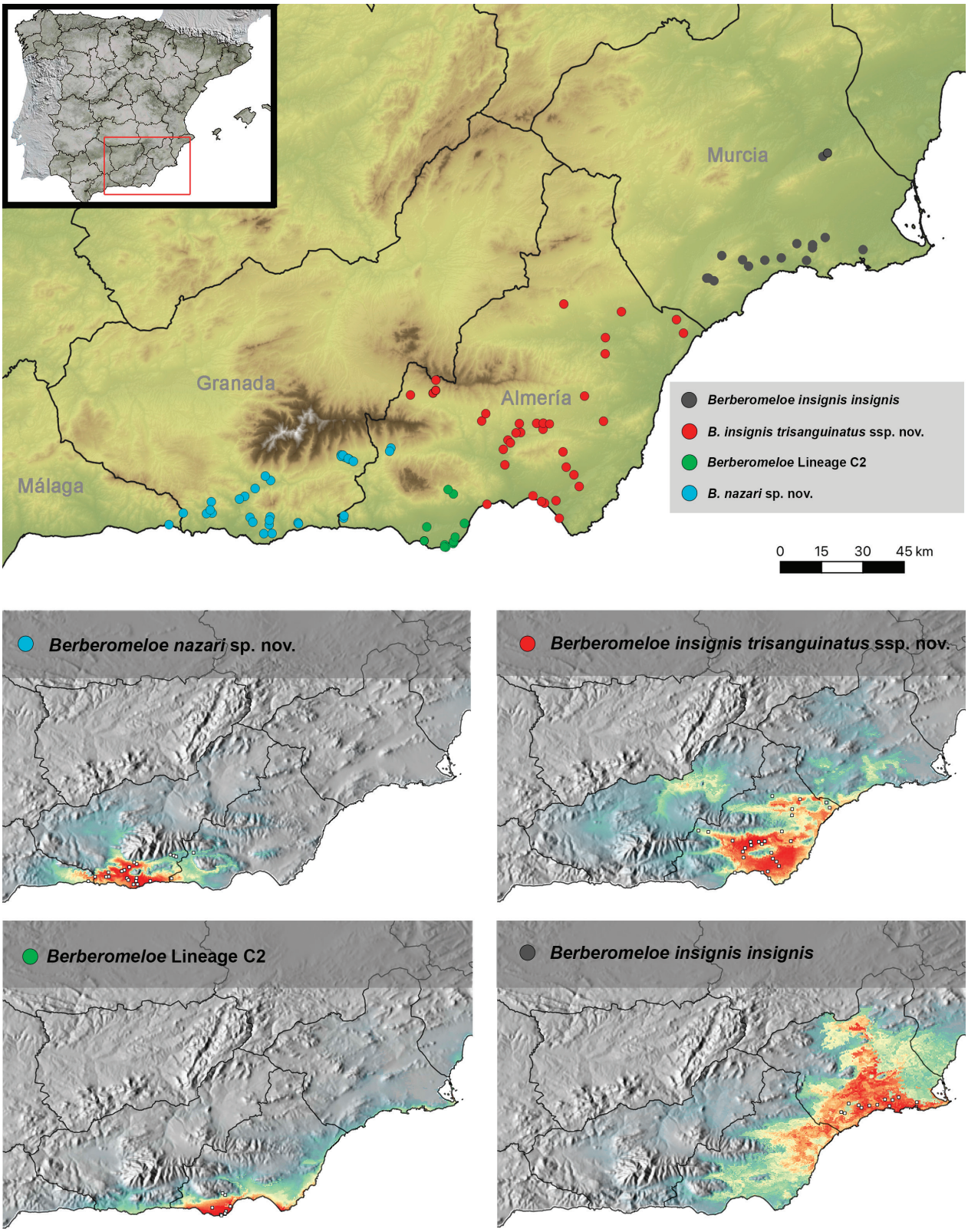

Figure 18. Geographic distribution records of *Berberomeloe insignis* sensu lato. Detailed information for each record can be found in Table S4. Potential distribution areas for each taxon are shown (see Material and methods for modeling details).

4. Discussion

4.1. Taxonomic novelty and species delimitation

Over recent decades, the rise of molecular techniques has catalyzed a wave of cryptic species discoveries, leading to a deeper understanding of biodiversity and speciation processes (Witt et al. 2006; Adams et al. 2014; Pérez-Ponce de León and Poulin 2016; Pola et al. 2023). The recognition of cryptic diversity is increasingly significant across a range of taxonomic groups (Dufresnes et al. 2019; Sainz-Escudero et al. 2022; González-Miguéns et al. 2020). However, species initially identified as cryptic may reveal distinct morphological traits upon closer examination (Horsáková et al. 2019; Korshunova et al. 2017; Pola et al. 2023), suggesting reconsideration of their cryptic, or rather, pseudocryptic, status.

However, our study emphasizes the need to explore morphological diversification in species that may not be cryptic but are incompletely revised (Cuesta-Segura et al. 2023; Recuero and Caterino 2024). Our findings indicate that morphological and genetic changes observed across the studied populations are not part of clinal variation, as evidenced by distinct and abrupt morphological differences between them. Split tree analysis supports the previous hypothesis regarding their phylogenetic relationships, revealing that the easternmost lineage is well differentiated from the others. While moderate to strong isolation by distance (IBD) signals are typically expected in populations subjected to high gene flow, our results show only a slight overall trend toward IBD. The low Mantel statistic indicates that genetic differences among lineages are not primarily driven by geographic distance. This observation underscores the likelihood that other processes, such as incipient speciation, play a significant role in the diversification of this group, especially given the high divergence observed between clades. Based on the evidence, we identified and described *B. nazari* **sp. nov.** and *B. insignis trisanguinatus* **ssp. nov.**

Our niche models show low overlap between *B. nazari* and other lineages, suggesting that it occupies a distinct climatic niche compared to the other taxa, including lineage C2 (Table 2; Figs S1, 18). The niche overlap among subspecies of *B. insignis* and the lineage C2 was relatively low to moderate, implying that while they share some climatic areas, notable ecological differences persist. Interestingly, despite phylogenetic and geographic proximity between *B. insignis insignis* and *B. i. trisanguinatus*, we did not observe specimens with intermediate characteristics that might indicate gene flow. This suggests that although these subspecies partially overlap in their climatic preferences, other factors, possibly ecological, behavioral, or genetic, may be maintaining their phenotypic differences near their contact zones.

In contrast, the absence of morphological differentiation and the presence of cyto-nuclear discordances in populations belonging to the lineage C2 highlight the need for further research to evaluate the extent of reproductive isolation among the involved lineages. At present, our data allow for outlining two alternative hypotheses that could explain the observed patterns of genetic and morphological discordances: (1) C2 populations would form a cohesive unit (sensu Coyne and Orr 2004), resulting from historical hybridization between lineages C and B, that led to an ancient mitochondrial capture, resulting in a hybrid species C2, with a closely related but differentiated C mtDNA lineage but with nuclear markers closely related to lineage B; Or, alternatively (2) C2 populations would not be cohesive, because they were the result of an old but still ongoing hybrid zone between lineage B2 and lineage C1, suggesting that B and C species coexisted in the region and that our sampling does not represent the extent of the ongoing hybridization. With our current sampling we cannot discriminate among these two alternatives. Further studies are needed to understand whether the processes described led already to speciation (hypothesis 1) or if we are facing a geographically unstable hybrid-zone (hypothesis 2). In the same geographic area, Andújar et al. (2012, 2014) presented a similar situation for the carabid beetle *Carabus baguenai* Breuning, 1926, a species resulting from ancient hybridization of nearly parapatric taxa, indicating that hybridization is not such a rare phenomenon in this geographic region. Since our data is incomplete we consider the C2 *Berberomeloe* problem still an open question for future research, and therefore, we refrain from making any taxonomic decisions regarding lineage C2. Additional sampling in zones between the ranges of *B. insignis* and *B. nazari*, combined with more robust genomic analyses (e.g., ABBA–BABA tests or F_{ST} estimates), will be necessary.

The addition of the newly described taxa in this study makes the province of Almería a focal point for *Berberomeloe* diversity (Fig. 18), including four taxa: *B. indalo*, *B. insignis trisanguinatus*, *B. nazari*, and *B. tenebrosus* (Sánchez-Vialas et al. 2020, 2023; this work). Most of these taxa exhibit parapatric distributions, with only *B. indalo* and *B. insignis trisanguinatus* found in syntopy at a few localities (García-París et al. 1999; this work). Even in a relatively small area such as the Sierra de Gádor, *B. tenebrosus* and the C2 lineage of *B. insignis* sensu lato, are parapatric, with the C2 lineage inhabiting lower altitudes (known populations found below 900 m a.s.l.) on southeastern slopes, while *B. tenebrosus* occupies higher altitudes (above 900 m, mostly between 1500 and 2000 m) on the western side (authors pers. obs.). A similar pattern is observed in Sierra de los Filabres, near Escúllar and El Haza de Riego, where *B. tenebrosus* and *B. i. trisanguinatus* occur less than 1 km apart. In this region, *B. tenebrosus* is confined to higher elevations and appears to be more common in its range (authors pers. obs.).

These findings present promising opportunities to study fine-scale ecological interactions across *Berberomeloe* lineages, particularly the potential roles of competitive exclusion or altitude-based habitat partitioning, highlighting the need for further research on the mechanisms shaping species coexistence. In this regard, to refine their distribution boundaries, further sampling is needed between Campo de Dalías/Sierra de Gádor and

La Rábita/Laujar de Andarax to the west (eastern limit of *B. nazari* and western limit of lineage C2, minimum distance: 29 km), and between Campo de Dalías/Sierra de Gádor and El Palmer/Aguadulce to the east (western limit of *B. i. trisanguinatus* and eastern limit of lineage C2, minimum distance: 12 km), to assess whether gradual phenotypic transitions occur. Similarly, additional sampling is needed for populations between the known localities of *B. i. trisanguinatus* and *B. i. insignis* (minimum distance: 18 km).

4.2. Secondary sexual traits and population divergence in *Berberomeloe*

The observed variation in male antennal morphology across distinct lineages of *Berberomeloe* suggests a potential role for sexual selection and reproductive isolation in driving divergence (Carson and Bryant 1979; Kawano 2003). Secondary sexual traits often evolve due to sexual conflict or mate choice (Andersson 1994; Fricke et al. 2010), which can establish reproductive barriers and ultimately contribute to speciation processes (Gavrilets 2014).

We identified distinct morphological extremes in male antennomere XI. Males of *B. nazari* have a wider antennomere, notched in its apical area (except some specimens of the C2 lineage), while *B. i. insignis* and *B. i. trisanguinatus* exhibit slender antennomeres, typically unnotched. Other antennomeres also show notable differences: X and VIII are significantly elongated in *B. i. insignis* compared to other taxa, while IX differs significantly across *B. i. insignis*, *B. i. trisanguinatus*, and *B. nazari*. Additionally, *B. nazari* has a shorter antennomere VII compared to the other taxa. Specimens from the C2 lineage exhibit a remarkable morphological variability in antennomeres XI and IX, along with head coloration, with antennal morphology overlapping that of *B. i. trisanguinatus* and *B. nazari*. A plausible explanation for the increased morphological variability in specimens from the C2 lineage is the existence of past or ongoing gene flow (Fuzessy et al. 2014; Enciso-Romero et al. 2017; Grant and Grant 2019). Notably, males and females of C2 show comparable variation, whereas in established species male variation is typically more constrained, likely due to sexual conflict or mate choice. This pattern suggests that C2 could represent a hybrid zone rather than a cohesive species and highlighting an avenue for future genomic investigation.

Male antennomeres V, VII, IX, and XI show a strongly dentate apical border on the inner side, covered by very short setae, distinct from the setae on the rest of the antennomere (authors pers. obs.). This specialized setation might play roles in searching for females, mate recognition, and courtship behaviors. In *Berberomeloe*, courtship begins with antennation, where males use their antennae to scrutinize the last female's abdominal tergites through vibratory movements (Bologna 1988). The variation in male antennae across these taxa may reflect adaptations related to mating behaviors, mate recognition, or environmental interactions (Greenfield 2002; Jayaweera and Barry 2017). However, non-adaptive processes, such as genetic drift, cannot be excluded. Field and experimental studies are needed to explore the behavioral and ecological significance of this antennal morphological diversity.

Female antennal morphology remains largely conserved, except in *B. i. insignis*, which shows marked differentiation in antennomeres VII, IX, and X. This elongation of antennomeres in females of *B. i. insignis* is particularly intriguing, especially given the apparent lack of selection pressures for antennal function in females, in contrast to the strong selection males face during mating.

4.3. Taxonomic boundaries and implications for conservation

The challenge of identifying and naming evolutionary units, whether intraspecific or at the species level, is crucial for raising awareness and ensuring the protection of distinct populations (Liu et al. 2022). Each unique lineage may harbor evolutionary traits that contribute to broader biodiversity, underscoring the need for precise taxonomic recognition. In this context, some populations might be distinct enough genetically or ecologically to warrant protection but do not yet meet the usual standards for species designation under commonly applied species concepts (i.e., due to the absence of clear reproductive barriers). Addressing this taxonomic challenge requires consideration of subspecific classification frameworks (Dufresnes et al. 2023, 2024). *Berberomeloe* presents a complex taxonomic situation due to its significant genetic and morphological diversity. The geographic proximity of the main units of *Berberomeloe*, along with the existence of narrow unsampled regions between them, suggests a predominantly parapatric distribution rather than clear allopatry. While parapatric taxa are often expected to show gradual phenotypic transitions due to gene flow (Mayr 1963), *Berberomeloe* instead exhibits sharp phenotypic distinction between units, suggesting potential barriers to gene flow or strong selective pressures maintaining these differences.

Conservation strategies should not only focus on taxa but also on protecting regions where key evolutionary processes – such as hybridization and local adaptation – drive and maintain biodiversity. Hybrid zones and other areas of ongoing diversification are crucial for preserving the mechanisms that generate evolutionary novelty and ecological resilience. This is particularly urgent in rapidly deteriorating landscapes such as southeastern Spain (Sánchez-Vialas et al. 2023). In this regard, Sierra de Gádor and its surroundings emerge as a critical focal area for conserving evolutionary processes in *Berberomeloe*.

Our findings emphasize the urgent need for intensified taxonomic exploration, even for taxa previously considered well-documented. Regions like Campo de Dalías and Sierra de Gádor, which are under severe threat from greenhouse expansion, highlight the critical importance of precise taxonomic identification to inform effective conservation efforts (Liu et al. 2022; Dufresnes et al.

2023; Recuero et al. 2023). Beyond their significance as centers of endemism, these areas also serve as key sites for understanding evolutionary processes, such as historical and ongoing hybridization. Preserving both the species and the evolutionary dynamics shaping them is crucial, reinforcing the need to integrate these factors into conservation planning.

5. Acknowledgements

We are grateful to Bernd Jäger (Museum für Naturkunde Berlin) for his invaluable comments on the historical type of *Meloe insignis*, and to Ivo Jurisch for kindly taking and sharing the photographs of it. We also thank Mercedes París and Alberto Rodríguez, curators of the entomological collections at the MNCN and MUNA, respectively, for their support in facilitating access to these collections. We are indebted to Alexandre François and Iñigo Esteban for providing samples and Jordi Tena, Marta Miñarro, and Helena Martínez for their assistance during field work. This study was funded by the project-grant PID2019-110243GB-100/AEI/10.13039/501100011033 (Ministerio de Ciencia e Innovación) to MGP and by the MNCN Grant "Premio Cabrera 2018" to ASV.

7. References

Adams M, Raadik TA, Burridge CP, Georges A (2014) Global biodiversity assessment and hyper-cryptic species complexes: More than one species of elephant in the room? Systematic Biology 63(4): 518–533. https://doi.org/10.1093/sysbio/syu017

Alcaráz F, Peinado M (1987) España semiárida: Murcia y Almería. In: Peinado Lorca M, Rivas-Martínez S (Eds) La Vegetación de España. Servicio de Publicaciones, Universidad de Alcalá de Henares, San Fernando de Henares, Madrid, pp. 257–281.

Andersson M (1994) Sexual selection. Princeton University Press, 624 pp.

Andújar C, Gomez-Zurita J, Rasplus JY, Serrano J (2012) Molecular systematics and evolution of the subgenus *Mesocarabus* Thomson, 1875 (Coleoptera: Carabidae: *Carabus*), based on mitochondrial and nuclear DNA. Zoological Journal of the Linnean Society 166(4): 787–804. https://doi.org/10.1111/j.1096-3642.2012.00866.x

Andújar C, Arribas P, Ruiz C, Serrano J, Gómez-Zurita J (2014) Integration of conflict into integrative taxonomy: fitting hybridization in species delimitation of *Mesocarabus* (Coleoptera: Carabidae). Molecular Ecology 23(17): 4344–4361. https://doi.org/10.1111/mec.12793

Bologna MA (1988) *Berberomeloe*, a new west Mediterranean genus of Lyttini for *Meloe majalis* Lineé (Coleoptera, Meloidae). Systematics and bionomics. Bolletino di Zoologia 55: 359–366. https://doi.org/10.1080/11250008809386633

Bologna MA (1991) Coleoptera Meloidae. Fauna d'Italia. XXVIII. Calderini, Bologna, 541 pp.

Cardelús B (1987) Naturaleza Ibérica. Radiotelevisión Española y Editorial debate, Barcelona, 221 pp.

Carson HL, Bryant PJ (1979) Change in a secondary sexual character as evidence of incipient speciation in *Drosophila silvestris*. Proceedings of the National Academy of Sciences 76(4): 1929–1932. https://doi.org/10.1073/pnas.76.4.1929

Charpentier T de (1818) *Meloë insignis*. Pp. 258. In: Germar EF (Ed) Vermischte Bemerkungen über einige Käferarten. Magazin der Entomologie 3: 228–260.

Coyne JA, Orr HA (2004) Speciation: a catalogue and critique of species concepts. In: Rosenberg A, Arp R (Eds) Philosophy of biology: an anthology. Wiley-Blackwell, 272–292.

Cuesta-Segura AD, Jurado-Angulo P, Jiménez-Ruiz Y, García-París M (2023) Taxonomy of the Iberian species of *Pseudochelidura* (Dermaptera: Forficulidae). European Journal of Taxonomy 860: 81–115. https://doi.org/10.5852/ejt.2023.860.2053

Darwell CT, Cook JM (2017) Cryptic diversity in a fig wasp community – morphologically differentiated species are sympatric but cryptic species are parapatric. Molecular Ecology 26(3): 937–950. https://doi.org/10.1111/mec.13985

de Queiroz K (1998) The general lineage concept of species, species criteria, and the process of speciation. In: Howard DJ, Berlocher SH (Eds) Endless Forms: Species and Speciation. Oxford University Press, 57–75.

de Queiroz K (2007) Species concepts and species delimitation. Systematic Biology 56(6): 879–886. https://doi.org/10.1080/10635150701701083

Dufresnes C, Beddek M, Skorinov DV, Fumagalli L, Perrin N, Crochet PA, Litvinchuk SN (2019) Diversification and speciation in tree frogs from the Maghreb (*Hyla meridionalis* sensu lato), with description of a new African endemic. Molecular Phylogenetics and Evolution 134: 291–299. https://doi.org/10.1016/j.ympev.2019.02.009

Dufresnes C, Poyarkov N, Jablonski D (2023) Acknowledging more biodiversity without more species. Proceedings of the National Academy of Sciences 120(40): e2302424120. https://doi.org/10.1073/pnas.2302424120

Dufresnes C, Ambu J, Galán P, Sequeira F, Viesca L, Choda M, Álvarez D, Alard B, Suchan T, Künzel S, Martínez-Solano I, Vences M, Nicieza A (2024) Delimiting phylogeographic diversity in the genomic era: application to an Iberian endemic frog. Zoological Journal of the Linnean Society 202(1): zlad170. https://doi.org/10.1093/zoolinnean/zlad170

Eberhard WG (1985) Sexual Selection and Animal Genitalia. Harvard University Press.

Enciso-Romero J, Pardo-Díaz C, Martin SH, Arias CF, Linares M, McMillan WO, Jiggins CD, Salazar C (2017) Evolution of novel mimicry rings facilitated by adaptive introgression in tropical butterflies. Molecular Ecology 26(19): 5160–5172. https://doi.org/10.1111/mec.14277

Fick SE, Hijmans RJ (2017) WorldClim 2: new 1km spatial resolution climate surfaces for global land areas. International Journal of Climatology 37(12): 4302–4315. https://doi.org/10.1002/joc.5086

Folmer O, Black M, Hoeh W, Lutz R, Vrijenhoek R (1994) DNA primers for amplification of mitochondrial cytochrome c oxidase subunit I from diverse metazoan invertebrates. Molecular Marine Biology and Biotechnology 3: 294–299.

Fricke C, Bretman A, Chapman T (2010) Sexual conflict. In: Wesneat DF, Fox CW (Eds) Evolutionary Behavioral Ecology. Oxford University Press, Oxford, UK, pp. 400–415.

Fuzessy LF, Silva IDO, Malukiewicz J, Silva FFR, Ponzio MDC, Boere V, Ackermann RR (2014) Morphological variation in wild marmosets (*Callithrix penicillata* and *C. geoffroyi*) and their hybrids. Evolutionary Biology 41: 480–493. https://doi.org/10.1007/s11692-014-9284-5

García-París M (1998) Revisión sistemática del género *Berberomeloe* Bologna, 1988 (Coleoptera, Meloidae) y diagnosis de un endemismo ibérico olvidado. Graellsia 54: 97–109. https://doi.org/10.3989/graellsia.1998.v54.i0.347

García-París M, Ruiz JL (2011) *Berberomeloe insignis* (Charpentier, 1818). Verdú, JR, Numa, C, Galante, E (Eds). Atlas y Libro Rojo de los Invertebrados de España (Especies Vulnerables). Vol. I. Dirección General de Medio Natural y Política Forestal. Ministerio de Medio Ambiente y Medio Rural y Marino, 285–294.

García-París M, Ruiz JL, Martínez-Solano I (1999) Primeros datos sobre la zona de contacto entre *Berberomeloe insignis* (Charpentier, 1818) y *B. majalis* (Linnaeus, 1758) en Almería (Coleoptera, Meloidae). Graellsia 55: 223–224. https://doi.org/10.3989/graellsia.1999.v55.i0.331

Gavrilets S (2014) Is sexual conflict an "engine of speciation"? Cold Spring Harbor Perspectives in Biology 6(12): a017723. https://doi.org/10.1101/cshperspect.a017723

González-Miguéns R, Muñoz-Nozal E, Jiménez-Ruiz Y, Mas-Peinado P, Ghanavi HR, García-París M (2020) Speciation patterns in the *Forficula auricularia* species complex: cryptic and not so cryptic taxa across the western Palaearctic region. Zoological Journal of the Linnean Society 190(3): 788–823. https://doi.org/10.1093/zoolinnean/zlaa070

Gower JC (1975) Generalized Procrustes Analysis. Psychometrika 40: 33–50.

Greenfield MD (2002) Signalers and receivers: mechanisms and evolution of arthropod communication. Oxford University Press, New York. https://doi.org/10.1093/oso/9780195134520.001.0001

Hewitt GM (1996) Some genetic consequences of ice ages, and their role in divergence and speciation. Biological Journal of the Linnean Society 58(3): 247–276. https://doi.org/10.1006/bijl.1996.0035

Hewitt GM (2000) The genetic legacy of the Quaternary ice ages. Nature 405: 907–913. https://doi.org/10.1038/35016000

Hijmans RJ (2017) geosphere: Spherical Trigonometry. R package version 1.5-10. Available at: https://cran.r-project.org/package=geosphere

Horsáková V, Nekola JC, Horsák M (2019) When is a "cryptic" species not a cryptic species: a consideration from the Holarctic micro-landsnail genus *Euconulus* (Gastropoda: Stylommatophora). Molecular Phylogenetics and Evolution 132: 307–320. https://doi.org/10.1016/j.ympev.2018.12.004

Huson DH, Bryant D (2006) Application of phylogenetic networks in evolutionary studies. Molecular Biology and Evolution 23(2): 254–267. https://doi.org/10.1093/molbev/msj030

ICZN (International Commission on Zoological Nomenclature) (1999) International Code of Zoological Nomenclature. 4th edn. International Trust for Zoological Nomenclature, London, xxix + 306 pp.

Jayaweera A, Barry KL (2017) Male antenna morphology and its effect on scramble competition in false garden mantids. The Science of Nature 104: 1–9. https://doi.org/10.1007/s00114-017-1494-0

Katoh K, Toh H (2008) Recent developments in the MAFFT multiple sequence alignment program. Briefings in Bioinformatics 9: 286–298. https://doi.org/10.1093/bib/bbn013

Kawano K (2003) Character displacement in stag beetles (Coleoptera: Lucanidae). Annals of the Entomological Society of America 96: 503–511. https://doi.org/10.1603/0013-8746(2003)096[0503:CDISBC]2.0.CO;2

Korba J, Opatova V, Calatayud-Mascarell A, Enguídanos A, Bellvert A, Adrián S, Sánchez-Vialas A, Arnedo MA (2022) Systematics and phylogeography of Western Mediterranean tarantulas (Araneae: Theraphosidae). Zoological Journal of the Linnean Society 196(2): 845–884. https://doi.org/10.1093/zoolinnean/zlac042

Korshunova T, Martynov A, Bakken T, Picton B (2017) External diversity is restrained by internal conservatism: new nudibranch mollusc contributes to the cryptic species problem. Zoologica Scripta 46(6): 683–692. https://doi.org/10.1111/zsc.12253

Kumar S, Stecher G, Li M, Knyaz C, Tamura K (2018) MEGA X: molecular evolutionary genetics analysis across computing platforms. Molecular Biology and Evolution 35(6): 1547–1549. https://doi.org/10.1093/molbev/msy096

Küster HC (1847) Die Käfer Europas. 12 Heft. Baner und Raspe, Nürnberg, pp. 83–84.

Liu J, Slik F, Zheng S, Lindenmayer DB (2022) Undescribed species have higher extinction risk than known species. Conservation Letters 15: e12876. https://doi.org/10.1111/conl.12876

López-Estrada EK, Asar Y, Sauquet H, Ho SY (2025) Unveiling the tempo of molecular and morphological evolution across the Tree of Life. bioRxiv 2025-07. https://doi.org/10.1101/2025.07.20.665814

López-Neyra CR (1914) Claves dicotómicas para la determinación de los meloideos indígenas. Boletín de la Real Sociedad Española de Historia Natural 14: 461–475.

Mayr E (1963) Animal Species and Evolution. Harvard University Press, Cambridge, Massachusetts, 814 pp.

Machordom A, Araujo R, Erpenbeck D, Ramos MA (2003) Phylogeography and conservation genetics of endangered European Margaritiferidae (Bivalvia: Unionoidea). Biological Journal of the Linnean Society 78: 235–252. https://doi.org/10.1046/j.1095-8312.2003.00158.x

Moritz C, Pratt RC, Bank S, Bourke G, Bragg JG, Doughty P, Keogh JS, Laver RJ, Potter S, Teasdale LC, Tedeschi LG, Oliver PM (2017) Cryptic lineage diversity, body size divergence, and sympatry in a species complex of Australian lizards (*Gehyra*). Evolution 72(1): 54–66. https://doi.org/10.1111/evo.13380

Oksanen J, Blanchet FG, Kindt R, Legendre P, Minchin PR, O'Hara RB, Simpson GL, Solymos P, Stevens MHH, Wagner H, Oksanen MJ (2013) Package 'vegan': Community ecology package, version 2: 1–295.

Olsen AM, Westneat MW (2015) StereoMorph: An R package for the collection of 3D landmarks and curves using a stereo camera setup. Methods in Ecology and Evolution 6(3): 351–356. https://doi.org/10.1111/2041-210X.12326

Palumbi SR, Martin AP, Romano S, McMillan WO, Stice L, Grabowski G (1991) The Simple Fool's Guide to PCR. Special Publ., Department of Zoology, University of Hawaii, Honolulu, 44 pp.

Padial JM, Miralles A, De la Riva I, Vences M (2010) The integrative future of taxonomy. Frontiers in Zoology 7(1): 1–14. https://doi.org/10.1186/1742-9994-7-16

Percino-Daniel N, Buckley D, García-París M (2013) Pharmacological properties of blister beetles (Coleoptera: Meloidae) promoted their integration into the cultural heritage of native rural Spain as inferred by vernacular names diversity, traditions, and mitochondrial DNA. Journal of Ethnopharmacology 147(3): 570–583. https://doi.org/10.1016/j.jep.2013.03.037

Pérez-Moreno I, San Martín AF, Recalde Irurzum JI (2003) Aportaciones corológicas y faunísticas sobre meloidos ibéricos (Coleoptera: Meloidae). Boletín de la Sociedad Entomológica Aragonesa 33: 195–217.

Pérez-Ponce de León G, Poulin R (2016) Taxonomic distribution of cryptic diversity among metazoans: Not so homogeneous after all. Biology Letters 12(8): 20160371. https://doi.org/10.1098/rsbl.2016.0371

Pfennig DW, Murphy PJ (2000) Character displacement in polyphenic tadpoles. Evolution 54(5): 1738–1749. https://doi.org/10.1111/j.0014-3820.2000.tb00717.x

Pfennig DW, Pfennig KS (2010) Character displacement and the origins of diversity. The American Naturalist 176(S1): S26–S44. https://doi.org/10.1086/657056

Phillips SJ, Anderson RP, Schapire RE (2006) Maximum entropy modeling for species geographic distribution. Ecological Modeling 190: 231–259. https://doi.org/10.1016/j.ecolmodel.2005.03.026

Phillips SJ, Dudík M, Schapire RE (2017) Maxent software for modeling species niches and distributions (v.3.4.1). Available at: http://biodiversityinformatics.amnh.org/open_source/maxent

Piñero FS, Tinaut A, Aguirre-Segura A, Miñano J, Lencina JL, Ortiz-Sánchez FJ, Pérez-López FJ (2011) Terrestrial arthropod fauna of arid areas of SE Spain: diversity, biogeography, and conservation. Journal of Arid Environments 75(12): 1321–1332. https://doi.org/10.1016/j.jaridenv.2011.06.014

Pola M, Tibiriçá Y, Cervera JL (2023) Psychedelics sea slugs: Observations on colour ontogeny in two nudibranch species from the genus *Nembrotha* (Doridina: Polyceridae). Scientia Marina 87(3): e072. https://doi.org/10.3989/scimar.05371.072

Posso-Terranova A, Andrés J (2018) Multivariate species boundaries and conservation of harlequin poison frogs. Molecular Ecology 27(17): 3432–3451. https://doi.org/10.1111/mec.14803

Postma E, van Noordwijk AJ (2005) Gene flow maintains a large genetic difference in clutch size at a small spatial scale. Nature 433: 65–68. https://doi.org/10.1038/nature03083

Pyron RA, O'Connell KA, Lemmon EM, Lemmon AR, Beamer DA (2020) Phylogenomic data reveal reticulation and incongruence among mitochondrial candidate species in Dusky Salamanders (*Desmognathus*). Molecular Phylogenetics and Evolution 146: 106751. https://doi.org/10.1016/j.ympev.2020.106751

Pyron RA, Kakkera A, Beamer DA, O'Connell KA (2024) Discerning structure versus speciation in phylogeographic analysis of seepage salamanders (*Desmognathus aeneus*) using demography, environment, geography, and phenotype. Molecular Ecology 33(2): e17219. https://doi.org/10.1111/mec.17219

R Core Team (2021) R: A language and environment for statistical computing. R Foundation for Statistical Computing, Vienna, Austria. URL: https://www.R-project.org

Recuero E, Etzler FE, Caterino MS (2023) Most soil and litter arthropods are unidentifiable based on current DNA barcode reference libraries. Current Zoology 70(5): 637–646. https://doi.org/10.1093/cz/zoad051

Recuero E, Caterino MS (2024) Hidden diversity in eastern North America: The genus *Ligidium* (Oniscidea, Ligiidae) in the southern Appalachian Mountains. Zoologica Scripta 53(5): 712–731. https://doi.org/10.1111/zsc.12661

Reyes-Velasco J (2024) A revision of recent taxonomic changes to the eyelash palm pitviper, *Bothriechis schlegelii* (Serpentes, Viperidae). Herpetozoa 37: 305–318. https://doi.org/10.3897/herpetozoa.37.e131965

Richards CL, Knowles LL (2007) Tests of phenotypic and genetic concordance and their application to the conservation of Panamanian golden frogs (Anura: Bufonidae). Molecular Ecology 16: 3119–3133. https://doi.org/10.1111/j.1365-294X.2007.03369.x

Rivas-Martínez S (1987) Memoria del mapa de las series de vegetación de España 1:400.000. ICONA, Madrid, 268 pp.

Rivas-Martínez S (2007) Mapa de series, geoseries y geopermaseries de vegetación de España [Memoria del Mapa de Vegetación Potencial de España. Parte I]. Itinera Geobotánica 17(1): 1–436.

Rodríguez-Flores PC, Jiménez-Ruiz Y, Forró L, Vörös J, García-París M (2017) Non-congruent geographic patterns of genetic divergence across European species of *Branchinecta* (Anostraca: Branchinectidae). Hydrobiologia 801: 47–57. https://doi.org/10.1007/s10750-017-3266-4

Sainz-Escudero L, Alonso M, Sánchez-Vialas A (2022) Diversity and distribution of Anostraca in temporary ponds in Western Africa with description of a new species of *Streptocephalus* Baird, 1852 (Pancrustacea: Branchiopoda: Streptocephalidae). Zootaxa 5213(4): 388–412. https://doi.org/10.11646/zootaxa.5213.4.4

Sánchez-Piñero F (2006) Fauna of Tenebrionidae in arid zones of SE Spain: Endemism and species turnover. Publications du Musée des Confluences 10(1): 121–126.

Sánchez-Vialas A, García-París M, Ruiz JL, Recuero E (2020) Patterns of morphological diversification in giant *Berberomeloe* blister beetles (Coleoptera: Meloidae) reveal an unexpected taxonomic diversity concordant with mtDNA phylogenetic structure. Zoological Journal of the Linnean Society 189(4): 1249–1312. https://doi.org/10.1093/zoolinnean/zlz164

Sánchez-Vialas A, Calatayud-Mascarell A, Recuero E, Ruiz JL, García-París M (2023) Predictions based on phylogeography and climatic niche modelling depict an uncertain future scenario for giant blister beetles (*Berberomeloe*, Meloidae) facing intensive greenhouse expansion and global warming. Insect Conservation and Diversity 16(6): 801–816. https://doi.org/10.1111/icad.12671

Sánchez-Vialas A, López-Estrada EK, Ruiz JL, García-París M (2024) Taxonomy of the West-Palaeartic *Lampromeloe* (Coleoptera: Meloidae) with the description of a new species. European Journal of Taxonomy 917: 19–49. https://doi.org/10.5852/ejt.2024.917.2385

Seehausen O, Takimoto G, Roy D, Jokela J (2008) Speciation reversal and biodiversity dynamics with hybridization in changing environments. Molecular Ecology 17(1): 30–44. https://doi.org/10.1111/j.1-365-294X.2007.03529.x

Selander RB (1966) A classification of the genera and higher taxa of the meloid subfamily Eleticinae (Coleoptera). Canadian Entomologist 98: 449–481. https://doi.org/10.4039/Ent98449-5

Settani C, di Giulio A, Finoia MG, Bologna MA (2009) Intra- and interspecific analysis of first instar larval morphology in the genus *Berberomeloe* Bologna, 1989 (Coleoptera: Meloidae). Zootaxa 2089: 52–64. https://doi.org/10.11646/zootaxa.2089.1.5

Taylor EB, Boughman JW, Groenenboom M, Sniatynski M, Schluter D, Gow JL (2006) Speciation in reverse: morphological and genetic evidence of the collapse of a three-spined stickleback (*Gasterosteus aculeatus*) species pair. Molecular Ecology 15(2): 343–355. https://doi.org/10.1111/j.1365-294X.2005.02794.x

True JR, Liu J, Stam LF, Zeng ZB, Laurie CC (1997) Quantitative genetic analysis of divergence in male secondary sexual traits between *Drosophila simulans* and *Drosophila mauritiana*. Evolution 51(3): 816–832. https://doi.org/10.1111/j.1558-5646.1997.tb03664.x

Valle F (2003) Mapa de Series de Vegetación de Andalucía. Rueda S.L., Madrid, 131 pp, 1 map.

Warren DL, Matzke NJ, Cardillo M, Baumgartner JB, Beaumont LJ, Turelli M, Dinnage R (2021) ENMTools 1.0: an R package for comparative ecological biogeography. Ecography 44(4): 504–511. https://doi.org/10.1111/ecog.05485

Witt JD, Threloff DL, Hebert PD (2006) DNA barcoding reveals extraordinary cryptic diversity in an amphipod genus: implications for desert spring conservation. Molecular Ecology 15(10): 3073–3082. https://doi.org/10.1111/j.1365-294X.2006.02999.x

Wooten JA, Gibbs HL (2012) Niche divergence and lineage diversification among closely related *Sistrurus* rattlesnakes. Journal of Evolutionary Biology 25: 317–328. https://doi.org/10.1111/j.1420-9101.2011.02426.x

Wright K (2006) Corrgram: plot a correlogram, R package, v.1.1. Available at: http://CRAN.R-project.org/package=corrgram

Wrzecionko A (2023) *Berberomeloe bubeniki* sp. nov. (Coleoptera: Meloidae: Lyttini) from Alicante Region, Spain. Studies & Reports-Taxonomical Series 19(2): 415–424.

Supplementary Material 1

Figures S1–S6

Authors: Sánchez-Vialas A, Calatayud-Mascarell A, Ruiz JL, Recuero E, García-París M (2026)
Data type: .docx
Explanation notes: Figure S1–S6. Environmental niche overlap comparisons.

Link: https://doi.org/10.3897/asp.84.e162254.suppl1

Supplementary Material 2

Tables S1–S5

Authors: Sánchez-Vialas A, Calatayud-Mascarell A, Ruiz JL, Recuero E, García-París M (2026)
Data type: .zip
Explanation notes: Table S1. Genetic distance matrix based on cox1 of *Berberomeloe insignis* sensu lato [xlsx file].

— **Table S2.** Data on specimens revised for qualitative and phenotypic traits [xlsx file]. — **Table S3.** Data on specimens used for antennomere morphometrics [xlsx file]. — **Table S4.** Recorded localities of the different taxa of *Berberomeloe insignis* sensu lato [xlsx file]. — **Table S5.** Summarised ANOVA results of the male and female

antennomeres VII–XI between *Berberomeloe* lineages [docx file].

Link: https://doi.org/10.3897/asp.84.e162254.suppl2